Enhancement of Maximum Power Extraction from a PV-Based Residential DC Microgrid under Partial Shading Conditions using Grey Wolf Algorithm

Gudina Fituma Birhanu

A Thesis Submitted to the Department of Electrical Power and Control Engineering

School of Electrical Engineering and Computing

Presented in Partial Fulfillment of the Requirement for Degree of Master's in Electrical Power and Control Engineering (Power system Engineering)

Office of Graduate Studies

Adama Science and Technology University

June, 2024

Adama, Ethiopia

Enhancement of Maximum Power Extraction from a PV-Based Residential DC Microgrid under Partial Shading Conditions using Grey Wolf Algorithm

Gudina Fituma Birhanu

Advisor: Prof.S Kim

A Thesis Submitted to the Department of Electrical Power and Control Engineering

School of Electrical Engineering and Computing

Presented in Partial Fulfillment of the Requirement for Degree of Master's in Electrical Power and Control Engineering (Power system Engineering)

Office of Graduate Studies

Adama Science and Technology University

June, 2024

Adama, Ethiopia

DECLARATION OF STUDENT

I hereby declare that this Master Thesis entitled "**Enhancement of Maximum Power Extraction from a PV-based residential DC Microgrid under Partial shading Conditions using Grey Wolf algorithm**" is my original work. That is, it has not been submitted for the award of any academic degree, diploma, or certificate in any other university. All sources of materials that are used for this thesis have been duly acknowledged through citation.

Gudina Fituma Birhanu

Name of Student	Signature	Date

RECOMMENDATION OF ADVISOR

I, the advisor of this thesis, hereby certify that I have read the revised version of the thesis entitled "**Enhancement of Maximum Power Extraction from a PV-based residential DC Microgrid under Partial Shading Conditions using Grey Wolf algorithm** prepared under my guidance by **Gudina Fituma Birhanu** submitted in partial fulfillment of the requirements for the degree of Master's of Science in Electrical Power and Control Engineering (Power Engineering). Therefore, I recommend the submission of a revised version of the thesis to the department following the applicable procedures.

Prof.S Kim ______ ____________________ ____________

Name of Advisor Signature Date

APPROVAL PAGE

I, the advisor of the thesis entitled "**Enhancement of Maximum Power Extraction from a PV-based residential DC Microgrid under Partial shading Conditions using Grey Wolf algorithm**" and developed by **Gudina Fituma Birhanu**, hereby certify that the recommendation and suggestions made by the board of examiners are appropriately incorporated into the final version of the thesis.

Prof.S Kim	____________________	____________
Name of Advisor	Signature	Date

We, the undersigned, members of the Board of Examiners of the thesis by **Gudina Fituma Birhanu** have read and evaluated the thesis entitled "**Enhancement of Maximum Power Extraction from a PV-based residential DC Microgrid under Partial Shading Conditions using Grey Wolf algorithm**" and examined the candidate during the open defense. This is, therefore, to certify that the thesis is accepted for partial fulfillment of the requirement of the degree of Master of Science in Electrical Power and Control Engineering (Power Engineering).

________________________________	________________________	________________
Chairperson	Signature	Date
________________________________	________________________	________________
Internal Examiner	Signature	Date
________________________________	________________________	________________
External Examiner	Signature	Date

Finally, approval and acceptance of the thesis is contingent upon submission of its final copy to the Office of Postgraduate Studies (OPGS) through the Department Graduate Council (DGC) and School Graduate Committee (SGC).

________________________________	________________________	______________
Department Head	Signature	Date
________________________________	________________________	______________
School Dean	Signature	Date
________________________________	________________________	______________
Office of Postgraduate Studies, Dean	Signature	Date

ACKNOWLEDGMENT

Prioritizing God above all, I would want to express my sincere gratitude to my advisor, Prof. S. Kim, for his invaluable guidance and assistance during the completion of my thesis. Thank you once more to the National Meteorology office staff for providing me with vital information for my study regarding Sululta's temperature and solar irradiance.

With immense pleasure, I express my gratitude to Tefera.T.Y (Ph.D) for his unwavering support, prompt responses, and availability during this research endeavor.

In conclusion, I express my gratitude to every one of my relatives and friends, especially Dugasa Getachew, for their amazing support and encouragement assistance during my coursework.

.

TABLE OF CONTENTS

LIST OF TABLES

LIST OF FIGURES AND ILLUSTRATIONS

LIST OF ACRONMYS AND ABBREVIATIONS

AC	Alternating Current
BD	Bypass Diode
BJT	Bipolar Junction Transistor
CPG	Constant Power Generation
D	Ratio
DC	Direct Current
DER	Distributed Energy Resource
DG	Distributed Generator
GA	Genetic Algorithm
GMPP	Global Maximum Power Point
GP	Global Peak
GWO	Grey Wolf Optimization
GW	Giga Watt
HC	Hill Climbing
HVAC	High Voltage Alternating Current
I	Current
IEC	International Electro technical Commission
IGBT	Insulated Gate Bipolar Transistor
LP	Local Peak
LVDC	Low Voltage Direct Current
MPP	Maximum Power Point
MPPT	Maximum Power Point Tracking
NOCT	Nominal Operating Cell Temperature
P&O	Perturb and Observe
PI	Proportional-Integral
PID	Proportional-Integral-Derivative
PV	Photovoltaic
P-V	Power-Voltage
PSC	Partial Shading Condition
PSO	Particle Swarm Optimization

PWM	Pulse Width Modulation
RE	Renewable Energy
SMPS	Switch Mode Power Supply
SP	Shading Pattern
TLBO	Teaching learning based Optimization
V	Voltage
WT	Wind Turbine
ZN	Ziegler Nichols

ABSTRACT

In recent years, the whole world is focusing on the utilization of solar energy because of the depletion of fossil fuels and its impact. However, PV system with multiple modules is exposed to non-uniform irradiance due to long building, trees, cloud, flying birds and etc. As the result, when certain section or parts PV modules receive different levels of sunlight, Partial Shading Condition (PSC) formed in the system. This leads to overall power loss and multiple peaks in Power-Voltage (P-V) characteristics curve. Multiple peaks in the P-V curve resulted when unshaded and shaded modules operate at different voltage during shadowing, which gives difficulty to extract maximum power from the PV system. In this condition, conventional maximum power point tracking (MPPT) algorithms like Perturb and Observe (P&O), may fail to track the global peak of P-V curve. To extract the maximum power generated by a PV device in this complex condition, improved MPPT approach needs to be applied. Thus, this thesis proposed Grey Wolf Optimization (GWO) algorithm to extract maximum available power under PSC, for a residential DC load micro grid. The GWO algorithm is utilized to find the best duty cycle for DC-DC boost converter in the PV system to adjust the maximum operating point among local and global peaks of PV curve. It inspired from the social hierarchy and hunting habits of grey wolves. In this study, centralized (single) MPPT controller configuration has been used to process power of the PV panels. Mathematical modeling of minimum load with 105W up to 4300W peak load for residential DC microgrid, solar energy analysis depending on meteorological data, boost converter design and formulation of GWO and P&O techniques has been done. Performance of P&O algorithm and proposed algorithm is compared under four Shading Patterns by using Matlab/Simulink 2018a. The findings confirmed that the proposed system operated with less output power oscillation, faster tracking time, and higher efficiency than traditional P&O algorithm.

Keywords: Boost Converter, Duty cycle, Grey Wolf Optimization (GWO), Maximum Power Point Tracking (MPPT), Partial Shading, Perturb and Observe(P&O), Shading Pattern

CHAPTER ONE

1. INTRODUCTION

1.1 Background of the thesis

Nowadays with the significant growth of the world population, there is also industry expanding which in turn creates a large demand for energy requirement. So, conventional energy sources such as coal, natural gas, gasoline, fossil fuels, oil, and nuclear energy are extensively utilized to provide this world's energy needs (Jamiati, 2021).

However consumption of conventional energy uses is under pressure due to population growth and rising of living standard. Especially in developing country, it is highly used type of energy and due to expansion of activities that use energy in both developed and developing countries are ever increasing, the demand for this energy also rising. The two primary problems this phenomenon has caused are the depletion of the most easily accessible energy sources, namely oil, and the problem of global warming brought on by the dramatic increase in greenhouse gas emissions, such as carbon dioxide and methane. Therefore, nowadays all nations of world corners are concentrating on using renewable energy (RE) that is inexpensive, pollution-free, and well-managed to battle climate change and global warming (Windarko et al., 2021).

Renewable energy is energy that comes from natural resources like sunshine, wind, tides, and geothermal energy. It produces no emissions, is inexpensive, easy to maintain, and cheap running cost. Because of this, renewable energy appears to be the most effective solution for issues related to energy sustainability and the environment. Among these Renewable energy sources (RES), solar energy is the popular and has become the most attractive renewable energy source because of its availability. All most all renewable energy comes from solar radiation, either directly or indirectly (Kannan & Vakeesan, 2016).

Consequently, energy that originates directly from the sun is referred to as solar energy. Every day, the sun releases an enormous amount of energy onto Earth's surface that, if appropriately harnessed, can meet all of the planet's energy needs. This massive amount of energy can be produced by combining traditional turbines with concentrated solar thermal or photovoltaic (PV) systems (El Hammoumi et al., 2022).

A photovoltaic system (PV) can be created by converting solar energy into electrical energy through the use of photovoltaic cells, solar panels, or modules. It has the advantages of low maintenance requirements, cheap running costs, and environmental friendliness. In addition to it benefits, it has drawbacks, such as a fluctuating output power due to variations in temperature and radiation. Non-uniform radiation on the surface of modules is also caused by dust, clouds, and the shadows cast by trees, towers, and birds flying over them. This yields the condition of the module known as partial shading. Owing to these circumstances, common issues with PV use include the challenge of achieving stability and obtaining the greatest amount of power (Sara & Faulianur, 2019).

The current-voltage (I-V) characteristic of a solar module has a nonlinear connection that is highly dependent on the weather. The maximum power is generated when the PV module's output voltage and current both reach their maximum values. This point is defined as maximum Power Point (MPP). Therefore, a maximum power point tracking (MPPT) strategy is required to track this moment to operate the PV module at its maximum power point. A solar array's power-voltage (P-V) characteristic has a single peak power point under optimal or uniform solar radiation conditions, which is ideal (Suhardi et al., 2019).

However, when comes to the real condition, solar arrays comprise many modules which is series–parallel connections. Every solar array module coupled in series or parallel has the potential to experience sporadic non-uniform irradiance levels. These findings highlight the issue of partial shadowing, which has a substantial impact on power generation because of the shaded PV cell's voltage drop. In these circumstances, the partially shaded photovoltaic cells or modules are causing potential divergences in the generated current, which might result in hot spots. In a nutshell, the module is harmed by the shaded cells' tendency to release heat as a result of polarity inversion brought on by possible divergences between series-connected cells.

The most common method of reducing this damage is to connect a bypass diode (BD) in parallel with a photovoltaic (PV) module. A bypass diode is incorporated to redirect current away from a reverse-polarized cell. As a result, current flows via the PV modules linked in parallel even while the voltage across the PV modules connected in series changes. This led to the development of several peaks (Laxman et al., 2021).The Grey Wolf optimization approach has been used to get the most power possible from the PV module in these conditions.

1.2 Statement of the problem

To enhance the effectiveness of a PV array several PV modules connected in series to increase voltage and connected in parallel to increase current. However, due to obstacles around the cell, trees, clouds, flying birds, long buildings, and dust, all modules of the PV pattern do not receive solar irradiance uniformly. Consequently, partial shading occurs within the photovoltaic array, leading to reduced output current in the shaded modules due to localized heat, known as hot-spot, which even damages the PV module. This reduction in output current adversely affects the overall power generation. In order to avoid this damage, a bypass diode is installed at PV module terminal. However, the presence of partial shading and bypass diodes alters the behavior P-V curve of solar arrays. The shaded modules that are bypassed by diodes and unshaded modules are operate at different voltage levels. This results formation of multiple peaks in the power-voltage (P-V) characteristics curve; with several Local Peaks (LP) and a single Global Peak (GP). This results in the challenge when using the traditional MPPT method to operate the PV system at its maximum operating point. Based on a review of previous research, classical approaches for maximum power point extraction are efficient and easy to implement. However, in the partial shading condition, failure to track the right direction of perturbation, steady state fluctuation, and failure to track Global peak are the main limitations of the widely used conventional method. In this sense, many watts of power are lost as a result of these impacts. Therefore, to mitigate all these impacts, it is necessary to build an MPPT algorithm(s) that are comprehensive and suitable for a broad range of atmospheric conditions. Hence, in order to optimize the operating point of a PV system to the global power peak and minimize power losses associated with conventional approaches, the application of a specific metaheuristic method, known as Grey Wolf Optimization technique, is employed.

1.3 Objective

1.3.1 General Objective

The general objective of this thesis is to enhance the maximum power extraction from a PV-based residential DC microgrid under partial shading conditions using the Grey Wolf Optimization (GWO) algorithm.

1.3.2 Specific Objectives

- To develop a mathematical model of PV size-based DC load microgrid and Analysis of solar energy
- To design of a DC-DC boost converter
- To formulate grey wolf optimization and P&O algorithm for MPPT

- To model and simulate the proposed system on MATLAB SIMULINK software and compare the results between the two methods.

1.4 Significance of the study

The demand for utilizing of Photovoltaic cells is ever-increasing in all worlds. Because, they are a pollution-free, cost-effective, zero-emission process, and simply maintainable. However, besides its merits, the efficiency of a photovoltaic system has drawn pressing concern around the world. Hence, the significance of this thesis lies in its potential to improve energy harvesting efficiency, mitigate the effects of partial shading, enhance DC microgrid stability, contribute to MPPT technique advancements, provide a comparison of MPPT tracking methods, and offer scalability and applicability in PV systems operating in DC microgrids. These contributions are vital for promoting the widespread adoption of utilizing renewable energy sources and aiding in the shift to a future with more resilient and sustainable energy systems.

1.5 Limitations of the Study

This thesis focused on the enhancement of maximum power extraction from a PV-based residential DC microgrid under partial shading conditions using Grey Wolf Optimization (GWO) algorithm. However, the approach does not consider the utilization of power during night time when solar radiation is absent, resulting in a complete loss of power generation from the PV system. In addition, the thesis may rely on certain assumptions and simplifications to develop the mathematical model and perform the analysis. These assumptions may not fully capture the complexity and variability of real-world scenarios, which could affect the accuracy and applicability of the results.

1.6 Scope of the study

This study involved studying and implementing extracting maximum power from PV modules under partial shading conditions. Mathematical modelings of all solar arrays based on 4.3KW residential DC load design have been carried out. Integration of Grey wolf optimization and P&O algorithm with boost converter are applied to achieve best operating voltage at which maximum power can be extracted, and finally, proposed systems are validated using MATLAB software. For PV design, DC load estimation as well as solar energy analysis based on the Metrological data of Sululta city was conducted.

1.7 Organization of the Thesis

In this study, the influence of partial shading conditions, and the problem of extraction power from PV systems particularly, tracking of maximum power under the formation of multiple peaks investigated. As well as their mitigation technique is proposed. The thesis is organized into five chapters. The background of the study, statement of the problem, objectives, limitations of the study, and significance of the study are all included in the first chapter.

The second Chapter examines the PV Module and its formations, photovoltaic effect, and different types of PV cells. Moreover, solar panel characteristics, the Importance of the DC microgrid, solar radiation in Ethiopia, the type of residential DC Load, the difference between shading and unshaded modules, and its effect under the P-V curve are explained in this chapter. In addition, this chapter discusses several related papers on maximum power tracking under PSC. There is also a discussion on maximum power tracking techniques.

The third chapter discusses the data collection method, solar energy analysis, investigation of load, and load estimation. This chapter also describes the sizing of the PV module with load and the design of the boost converter. In addition, this chapter includes modeling of maximum power tracking techniques and problem formulation of the control system.

In chapter four, the MATLAB/SIMULINK model has been simulated with and without optimization techniques to identify the level of power extracted from PV under partial shading conditions. The performance of the proposed system with shading conditions, before and after MPPT techniques was discussed. In this line, the comparison between the grey wolf algorithm and the perturb and observe method has been discussed.

Chapter 5 outlines the conclusion developed based on the investigation results, as well as the recommendation provided on partially shaded PV-based DC microgrid system; and the future work to be done.

CHAPTER TWO

2. LITERATURE REVIEW

2.1 Introduction

The increasing adoption of Photovoltaic (PV) system in residential areas has led to emergency of DC microgrid, which offers numerous benefit such as improved energy efficiency, enhanced reliability and reduced carbon emission. In order to increase the utilization of solar energy further, it is crucial to optimize the power extraction from PV based residential DC microgrid. This optimization process involves finding the optimal operating points for PV system considering factors such as radiation of sunlight.

The goal of this study is to employ grey wolf algorithm in maximizing power extraction from PV based residential DC microgrid. It is expected to achieve better results compared to conventional optimization technique. It involves developing mathematical model of PV system considering such as radiation of sunlight, temperature and load variation. Moreover, this chapter describes about basics of PV model, solar energy in Ethiopia, importance of DC microgrid, PSC of module and its effect, characteristics of solar cell and MPPT methods used in the thesis.

2.2 Solar Energy in Ethiopia

Apart from geothermal and tidal energy, sunlight is the ultimate power source and the primary energy provider for all living organisms; even the energy contained in fossil fuels has its ultimate source in the sunlight. It releases massive amounts (millions of kWh) of energy into space every hour (Benti et al., 2022).

The sun is an example of a typical star, with an estimated weight of 2060 kg, 700 thousand km of beam length, and an estimated lifespan of 5 billion years. It has an approximate surface temperature of 5800 Kelvin and an approximate interior temperature of 15 million Kelvin. The sun gets its high temperature from reactions that are based on the nuclear fusion process, which converts hydrogen to helium. The large amounts of energy that the sun receives and continuously emits are what allow it to keep a steady energy balance and a temperature that is conducive to life (Hailu et al., 2021).

Ethiopia has major topography fluctuations result in a tropical monsoon climate. The middle mountain range, with its high plateau morphology, is divided by the Great Rift Valley. Hence, in Ethiopia, energy from sun is the most promising opportunity for distributed energy as well as alternative energy sources.

According to different studies, solar radiances vary significantly during the year, ranging from a minimum of 4.54 kWh/m2 in July to a maximum of 6.66 kWh/m2 in February and March.

2.3 Concept of residential DC microgrid

A microgrid is a power distribution system that integrates controllable loads with distributed energy resources (DERs). Microgrids can be utilized in two ways: either they can be used to supply loads independently of the main grid by using DERs (i.e. remote area), or they can be supplied to the main grid. It is often utilized as a crucial component to integrate DER and lower transmission losses for efficiency. It can also accepted as to a small-scale grid (Chauhan et al., 2018).

To get AC electricity from the central station to the residences and commercial buildings that use it for AC motors, incandescent lights, and other AC equipment for heating and cooling, the conventional electric power system was developed. Lower-voltage distribution lines and high-voltage AC (HVAC) transmission lines were used for this application. In the meanwhile, DC power systems are employed in industrial power distribution networks, telecommunications networks, long-distance or maritime cable point-to-point transfers, and the linking of AC grids operating at various frequencies.

A transmission and distribution network carries the power from generation station to consumer in a conventional system in a single direction. Power flow is now possible in two ways due to the increasing availability of distributed energy resources (DERs) such as battery systems, rooftop PV systems, small wind turbines (WTs), and other types of DERs. This led to the emergency of microgrids which can sell back excess power to the main grid or use as power source in the remote area or islanded mode. Depending on the use, a microgrid's size can change. Most of the time, idea of a microgrid, for instance, can be applied to a, smart building, or smart house (Chauhan et al., 2018).

2.3.1 Importance of PV-based DC microgrid

Developments in power electronics have a big impact on development of DC microgrid-based renewable energy sources like PV. Due to the quick advancement of DC technology, nowadays DC loads use less energy than AC loads. DC output power from PV systems can be used straight away without being converted into an low DC voltage. PV-based DC microgrid offer advantages in multiple directions, despite the fact that their size varies according to their intended use.

If there are any electrical losses in the DC system, there are no skin, capacitive, or inductive effects. Compared to the AC system, it has better voltage regulation because the steady state is not affected by an inductive effect. This technique also eliminates power loss that arises from the charging and discharging of capacitors. Therefore, it has minimal power loss. The absence of the skin effect allows the DC system to utilize the entire line conductor's cross-section area. In DC systems, it permits the use of a thinner conductor by reducing the conductor weight.

The DC system has less potential stress than the AC system at a given voltage. The voltage level aids in reducing the gap that exists between the two conductors of the distribution line. In proportion to the conductor's weight and potential stress, the tower and insulator sizes should be lowered. Consequently, the system's cost decreases and affordability increases.

In this system also calculation of system analysis has been reduced due to the absence of components of inductive and capacitors.

DC power is necessary for the operation of the majority of appliances, including Laptops, fluorescent lights, and various machinery and equipment used in industry.

Nowadays, they need to convert the available AC power into DC in order to function internally to use DC power, and most of these conversion stages usually involve inefficient rectifiers and input transformers. Additionally, for example, the electricity from solar panels needs to be converted to AC to connect to the current AC electrical grid, and then it needs to be converted back to DC for a large number of end users. So, significant energy losses are associated with these DC-AC-DC power conversion stages. As a result, expanding the DG-based DC microgrid will mitigate these losses and increase system reliability and efficiency while disregarding all of the aforementioned losses (Chauhan et al., 2018).

Due to benefits like increased efficiency and dependability, sustainability, the greenhouse effect, lack of waste, no need for expensive long transmission lines, fewer conversion stages, and uninterrupted power delivery over traditional ac systems, there has been a lot of research conducted recently on PV-based residential microgrid systems. Due to these, applications of DC systems in residential areas becoming increasing.

2.4 Selection of DC voltage level for home appliances

A distributed energy source system, an energy storage device, and loads make up a DC house. Line regulating converters are utilized to link the sources to a DC bus. In situations where a load's operational voltage matches that of the bus, it has a direct connection to the bus; in other situations, a load converter is used (Sabry et al., 2020).

Choosing the appropriate voltage level is one of crucial steps in establishing a DC household system configuration. The voltage levels utilized for DC residential systems are known with the absence of clear standardization (Pfuno & Mathew, 2018).

The elements that serve as the primary design criteria are determining the distribution voltages that are used for various solutions. For example, the car industry uses 12V distribution systems. However, the advancements in electrical technology in modern cars result in increased electricity use. This is why the voltage level was increased to 24-48 in order to decrease conductor size and increase efficiency. Many low-power electrical devices in homes can be safely powered at this voltage level. But, appliances with medium power consumption can be powered by 230–400 V. There is no discernible increase in efficiency over 400V, at which point the protection system starts to show vulnerabilities (Rodriguez et al., 2015).

Data centres can distribute power using voltage levels between 380 and 400 V DC. Because this voltage level has been tested using a unipolar model in several applications. For example, 48 V DC can be used to efficiently distribute power up to several hundred watts. This would cover devices with low power consumption. In order to reduce distribution losses, an increase in voltage is inevitable; as a result, more robust protective mechanisms must be created (Moussa et al., 2018).

According to a number of studies, the efficiency gain from using 380 V DC to power high-power loads such stoves and mitad is just 0.3% higher than that of 120 V DC. As well as the potential danger from an electrical shock is reduced because 120V DC is considered an extra-low voltage. Additionally, a number of studies show that 48–120 VDC systems effectively distribute energy for residential applications (Rodriguez et al., 2015).

Various International organizations are drafting the necessary regulations to establish DC systems for residential and building applications.

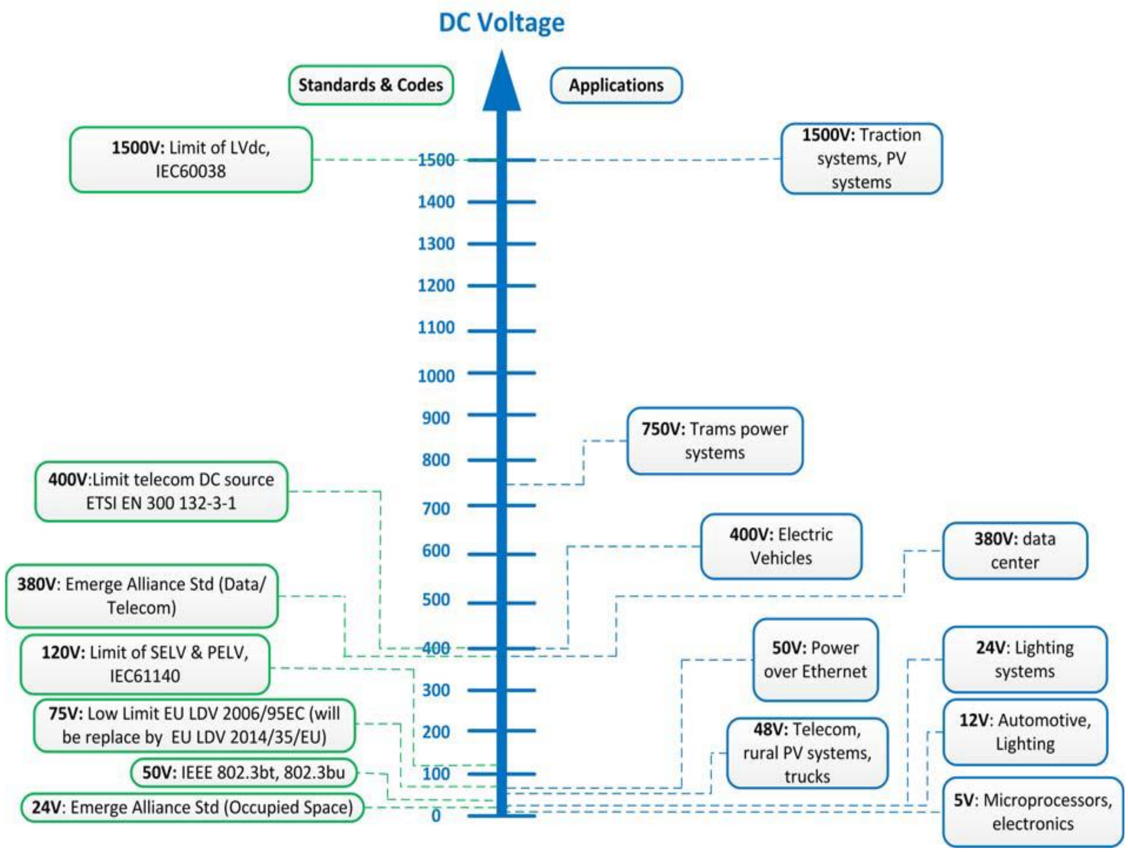

Figure 2.1 DC voltages applications and Standards codes (Rodriguez-Diaz et al., 2016)

2.5 Basic of PV module

A photovoltaic module, sometimes referred to as a solar panel or PV module is a set of connected solar cells that combined to generate energy from sunlight. It is the fundamental component of a solar power system. The part that directly interacts with sunlight to produce electricity is the photovoltaic module. It made from semiconductor materials like silicon (Si) and gallium (ga).

2.5.1 Photovoltaic effect

A junction is formed when two materials of different n-types and p-type come together, as shown in Figure 2.2. There are a lot of electrons in the n-type substance. Consequently, the electrons from the n-side move in the direction of the holes in the p-material when they come in contact. As a result, in the area around the junction, the n-material acquires a positive charge, and the p-material a negative charge. When the junction potential achieves an equilibrium value, carrier diffusion continues and the flow of holes and electrons in both directions is equal. This state is referred to as the p-n junction's unbiased condition. .

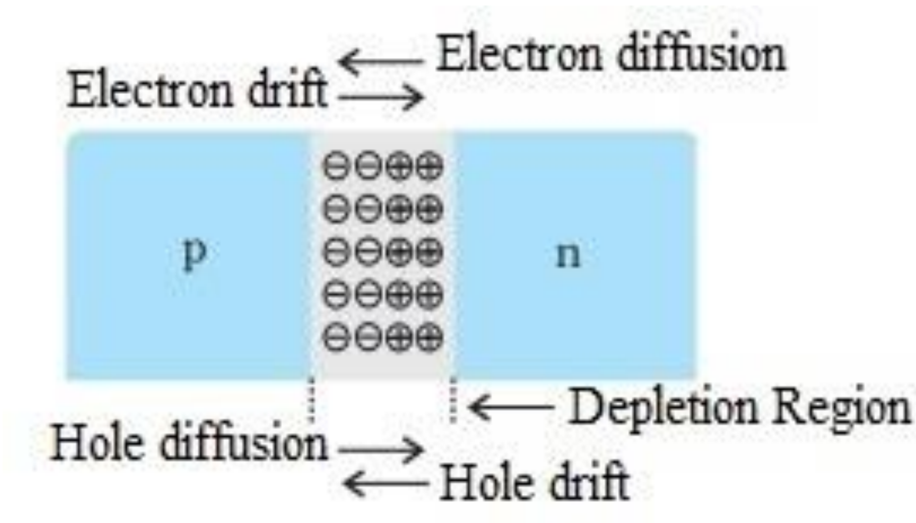

Figure 2.2 Formation of P-N Junction (Heng, 2024)

An electric field is created at the interface between the p-type and n-type layers, forming a "cell section (junction)." A percentage of the photons that enter a solar cell more especially, p-n junctions are absorbed inside the junction area. Then silicon crystal's electrons are freed as a result of this absorption process.

Electrons will be able to pass through the silicon and enter an external circuit if photon energy is high enough to overcome the electric field created at the junction. In this case, the electric current flows in the opposite direction as when the device operates as a diode.

Figure 2.3 explains the operation of solar cells briefly.

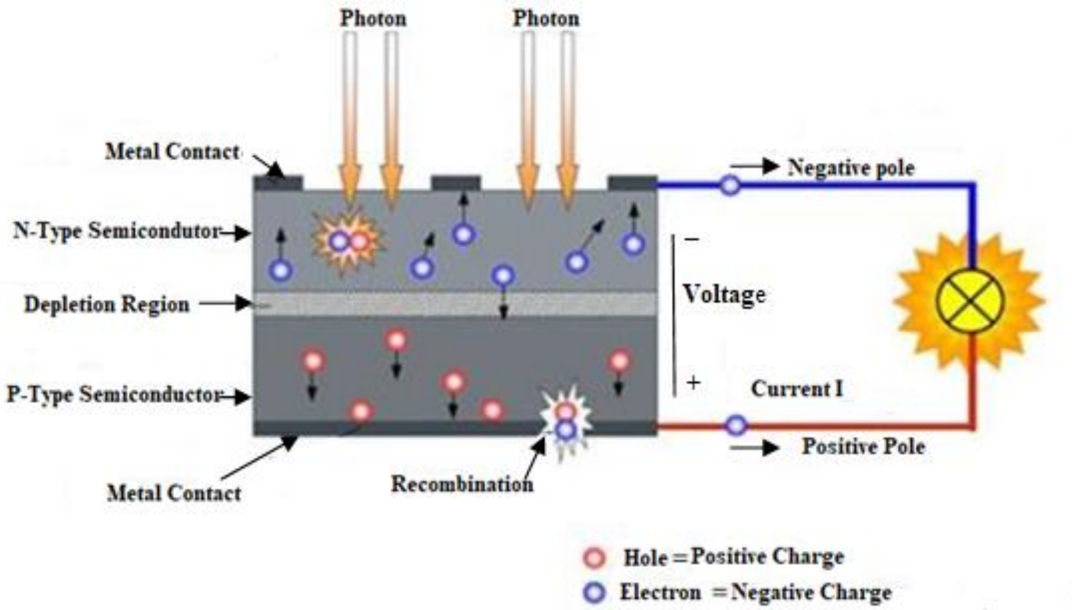

Figure 2.3 Operation of solar cell (Rathod et al., 2022)

2.6 Main PV cell type

Depending on raw material used to make them and the specific method used in their manufacture, silicon photovoltaic cells can be categorized into four groups.

1. **Silicon with a single crystal**; the fundamental component is silicon single-crystalline. They are created by purifying, melting, and crystallizing silicon into ingots. Single cells are formed by slicing the ingots into thin wafers. Although it is the most established and costly production method, solar conversion technology is still the most effective and commonly utilized. The effectiveness of the cells varies from 14% to 18%.
2. **Poly-crystalline;** the size of this particular cell is huge in size and is readily shaped into a square, thus there is almost no dead space between cells. In comparison to single crystalline, it has marginally lower conversion efficiency, but its manufacturing costs are also cheaper. The efficiency of cells varies from 10% to 13% (Rathore et al., 2021).
3. **String Ribbon:** This is an improvement on the synthesis of poly-crystalline silicon. Costs are significantly cheaper because there is less labor involved in its manufacturing. Average cell efficiency ranges from 8% to 10%.

4. **Technology that uses thin-film solar cells:** one or more thin layers of photovoltaic material and materials like glass, plastic, or metal substrate is used to create second-generation thin-film solar cells. Thin-film technologies use a variety of materials, including micro/nanocrystalline silicon (mc-Si), amorphous silicon (a-Si), and CdTe. These materials are all characterized by a direct band gap, which permits very effective light absorption even at very low thicknesses. With silicon thin-film technology, a triple junction device can achieve an efficiency of this cell up to 14.0% (Righini& Enrichi, 2019).

Temperature's impact on solar cells

As temperature rises, cell efficiency decreases. Crystalline cells are more heat-sensitive than thin-film cells. Output of crystalline cells decreases by around 0.5% for every degree Celsius as the cell's temperature rises. Due to the fact that amorphous silicon cells lose about 0.2% of their output for every degree Celsius that they increase in temperature. Therefore, modules should be maintained as cool as possible (Adeeb et al., 2019)(Karakilic et al., 2022).

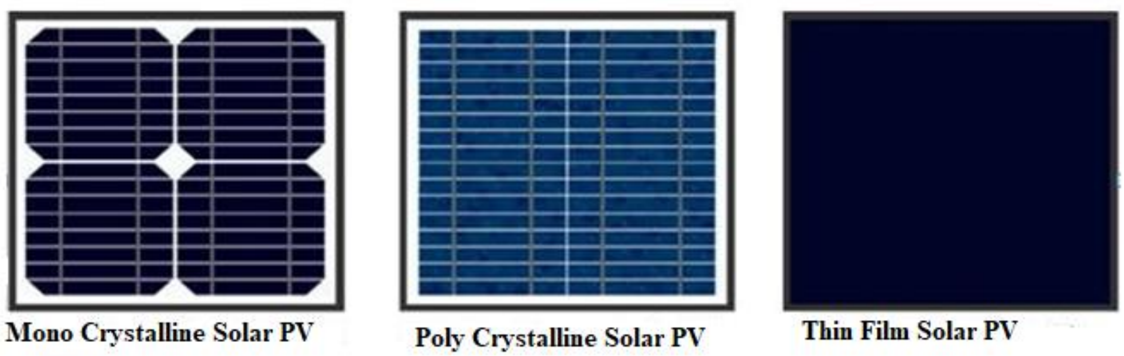

Figure 2.4 Types of PV cells (El Hammoumi et al., 2022)

2.7 Equivalent Circuit of PV Cell and Its characteristics

The electrical analysis of the system approximates the PV circuit as a continuous current source. To understand the complex physical process occurring in the PV cell, it is represented by the equivalent electrical circuit displayed in Figure 2.5. The following criteria need to be taken into account. The current, I at the output terminals is equal to the current generated from light Ipv, minus the diode current Id and the shunt leakage current Ish.

The other term is the series resistance (Rs) which internally hinder the flow of current in the output terminal of PV cell. It is dependent on contact resistance, contaminants, and the depth of the p-n junction. The PV conversion efficiency is not affected by changes in Rsh, although it is sensitive to little variations in Rs. A slight increase in Rs can have a substantial negative impact on PV output (Ciocia et al., 2020).

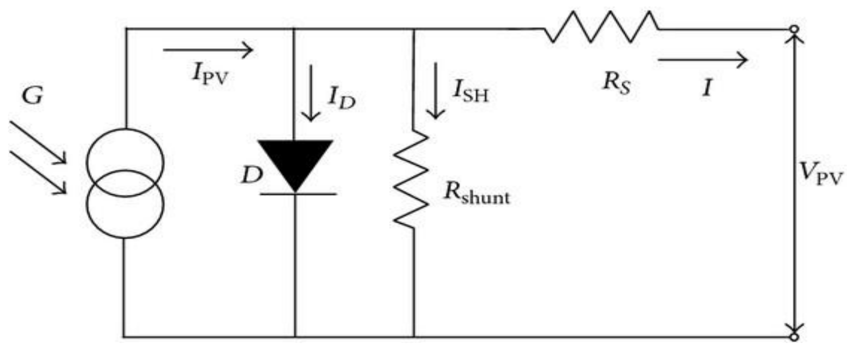

Figure 2.5 Equivalent electric circuit of PV cell (Ciocia et al., 2020)

When the load current is zero, the open circuit voltage of cells, or Voc, is determined by the following.

$$Voc = Io(I_{PV} - I_D)R_{sh} \tag{2-1}$$

Conventional diode current expression will be;

$$I_D = I_O \left[\exp\left(\frac{qVoc}{AKT}\right) - 1\right] \tag{2.2}$$

Where Io is the saturation current of the diode (A), q is electron charge (1.6×10–19C), A is curve fitting constant, k is Boltzmann constant (1.38×10–23J/°K), T is Temperature on absolute scale in K°.

Thus, the load current is given by the expression;

$$I = I_L - I_O exp\left[\left(\frac{qVoc}{AKT}\right) - 1\right] - \frac{Voc}{Rsh} \tag{2.3}$$

The leakage current to the ground is the final term. When leakage current compared to I_L and Io, it is insignificant in practical cells. Furthermore, it ignored.

When discussing the electrical performance of PV cells, the two most significant figures of merit that are frequently employed are the open circuit voltage (Voc) and the short circuit current (Ish) under full light. By shorting the output terminals and measuring the terminal current, the short circuit current can be determined. Under these conditions, the photocurrent I_L is the short circuit, ignoring the modest diode and ground leakage current at zero voltage. When ground leakage current is neglected, the maximum voltage generated at open circuit voltage is;

$$Voc = \frac{AKT}{q}\frac{(Ipv)}{Io} + 1 \qquad (2.4)$$

2.7.1 I-V and P-V Curves

The relationship between the current and voltage output of a PV cell under various operating conditions is shown by the I-V curve in Figure 2.6. It describes the distinctive nonlinear character of cells. Usually, the origin, where the voltage and current are both zero, is where the curve begins. The current rises in tandem with the voltage until it reaches the short-circuit current (Isc), or maximum value. Since the cell is now shorted, there is no voltage across it.

The current gradually drops as the voltage rises until it approaches zero, which is the open-circuit voltage (Voc). The maximum power point or operating point is where the output power of cells is maximized and it is important concept to understand from the I-V curve.

By showing the relationship between the power output and the voltage across the PV cell, the P-V curve completes the I-V curve. The calculation of power output involves multiplying the voltage and current. The PV cell can produce its maximum power output at the MPP where the product of voltage and current is maximal. For PV systems to operate as efficiently as possible, two critical parameters that must be determined from the P-V curve are Vmpp and Impp.

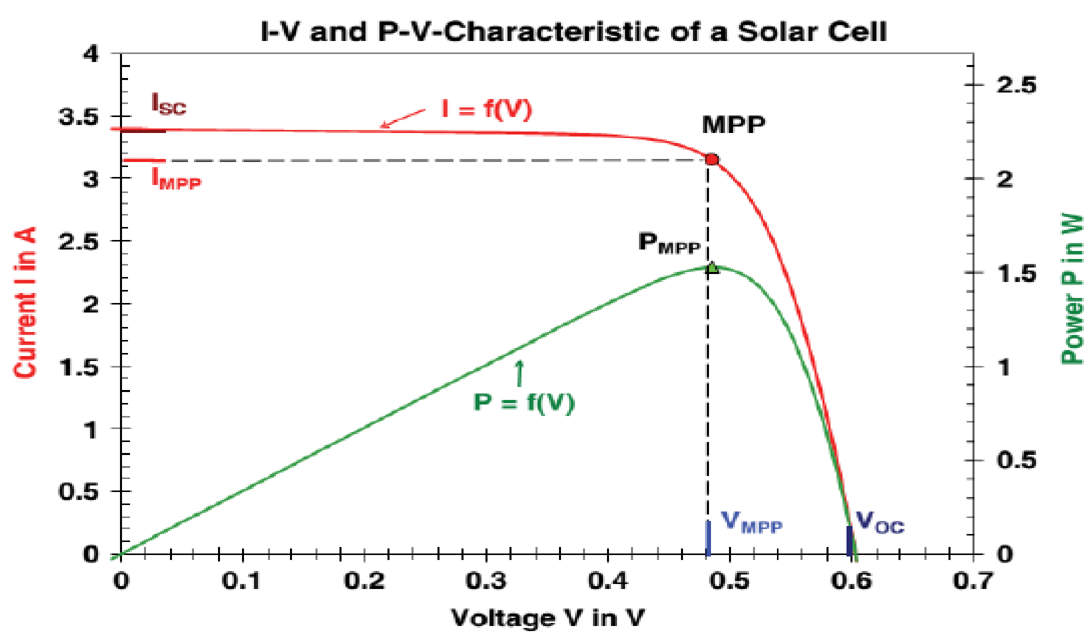

Figure 2.6 I-V and P-V solar cell characteristics without shading (Dambhare et al., 2021)

In ideal or uniform solar radiation case, a power-voltage (P-V) characteristic of solar array has single peak power as shown in Figure 2.6. However, under partial shading, P-V characteristic of solar array will have multiple peaks since different PV module operates at different operating voltage.

2.8 Partial Shading Condition and Its effect

Partial shading Condition refers to situation in which certain section or parts of a Photovoltaic (PV) module or array receive different levels of sunlight or shading. When PV module or array is subjected to partial shading, overall performances and power output of the system can be significantly affected.

A number of things, including surrounding structures, trees, clouds, and even the sun's angle, can provide partial shadowing. Figure 2.7 shows practical shading of PV module.

Figure 2.7 Partial shading on the rooftop PV module (Tzikas et al., 2017)

When shading occurs on the PV module, it interrupts the uniform absorption of sunlight across the surface, resulting in a mismatch in the generated current and voltage. The major challenge with partial shading is that the PV module is typically interconnected in serious and parallel configurations to meet desired voltage and current requirements. In serious configuration, if one module experiences shading, it can limit the current flow through the entire string, reducing the overall power output. In a parallel configuration, shading can cause significant voltage differences between shaded and unshaded modules, leading to imbalanced power generation.

To prevent impact of shading, numerous technique and methods have been developed. One popular method involves connecting individual modules in parallel to a bypass diode. Bypass diode allow current to allow around shaded modules minimize in the power reduction brought on by shadowing.

Another approach is the use of tracking maximum power point tracking algorithm, which continuously monitor the operating point of the PV system to enhance the power generation. The algorithms help to optimize the output power from the system with shading condition by dynamically adjusting the operating voltage and current.

Generally, partial shading condition pose a challenge to the performance of PV system as they can lead to power loss and reduced efficiency. However, through the implementation of bypass diode, MPPT algorithms, and others shading mitigation techniques, impact of partial shading can be minimized, allowing for improved overall performance and power extraction from the PV system. In this study enhancement of maximum power extraction residential DC microgrid based partially shaded PV modules has been carried out by using Grey wolf algorithm and perturb and observe algorithm. In this line the performance comparison between two methods as conventional method and non-conventional method are has been discussed. The effect of bypass diode and shading on P-V characteristics of solar cells are clearly shown on Figure 2.8.

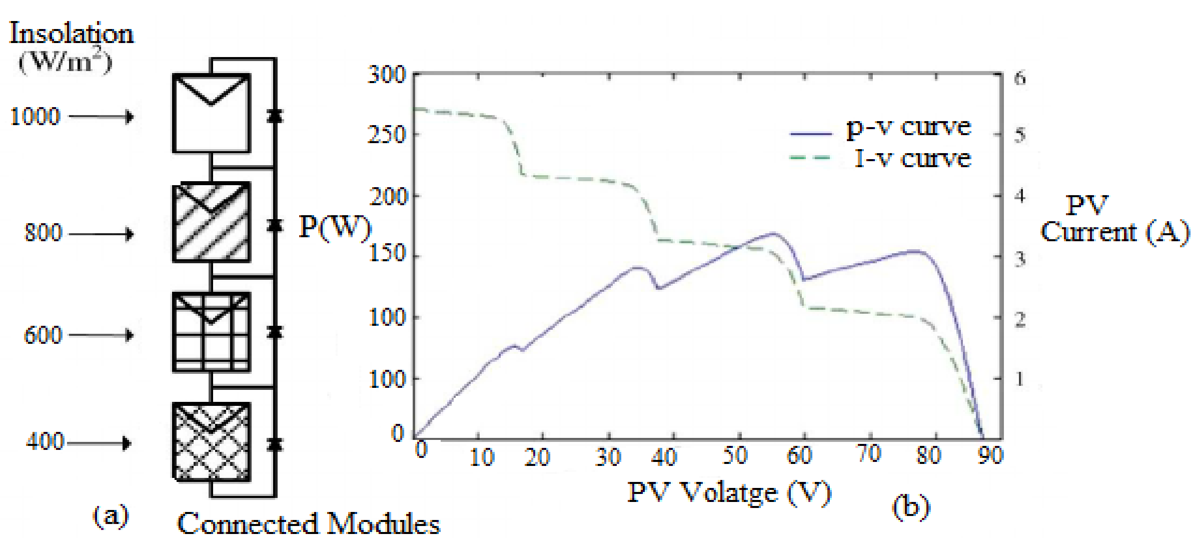

Figure 2.8 (a) PV module with partial shading condition, (b) P-V and I-V curve of PV array (Chen et al., 2014)

2.9 Methodology of the system

In this study, PV system with Central MPPT has been applied for DC microgrid Load. PV modules are designed under Partial Shading Conditions due to different reasons such as clouds, long trees and buildings and even the gradual motion of the sun. Thus, several components or units are combined in order to fulfill the study's purpose. The MPPT algorithm with a boost converter based on GWO is designed to extract the maximum power of a solar module by dynamically adjusting the operating point to the maximum power. The current and voltage obtained from the shaded PV module are given to the MPPT Controller. Then the measured value is fed to the MPPT controller to determine and monitor the best duty cycle for optimum operation voltage.

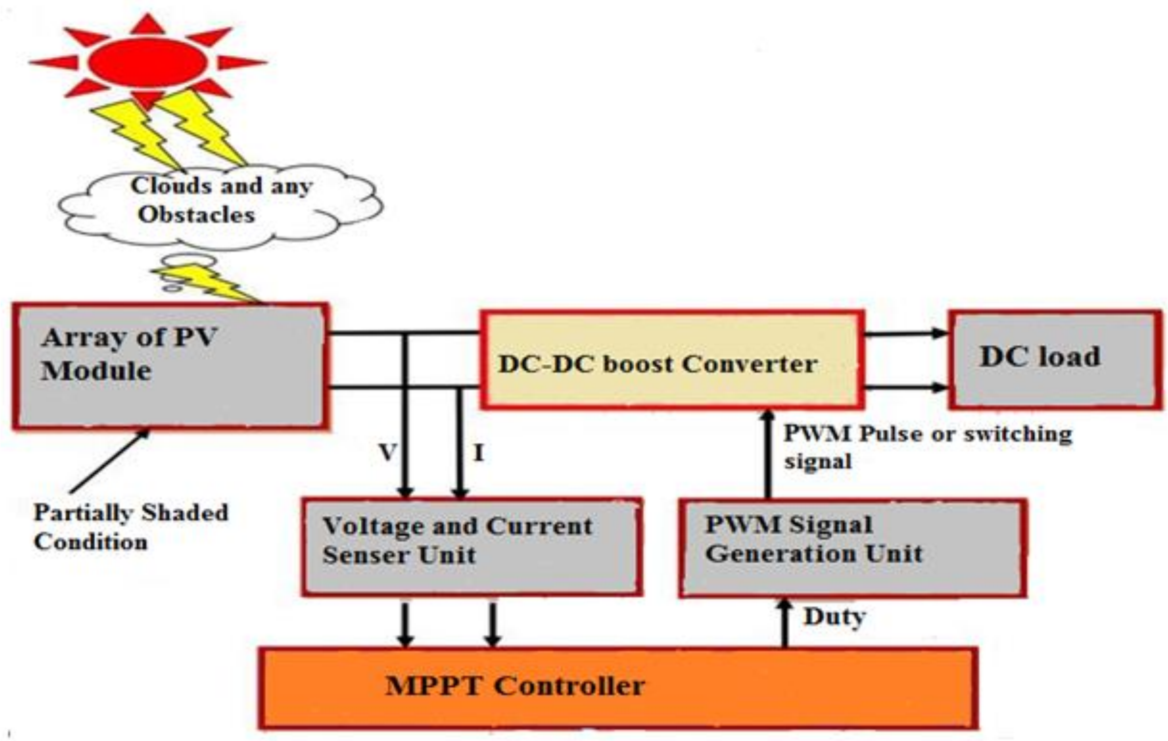

Figure 2.9 System with proposed MPPT controller (Neethu & Senthilkumar, 2020)

The Proposed system consists following component;

- PV Panel
- Voltage and current sensor unit
- MPPT Controller
- PWM Generation Unit
- Boost Converter

- DC-Load

2.9.1 PV module

Photovoltaic (PV) systems are popular among the rapidly expanding energy producing devices in the modern energy sector. Due to their capacity to lower greenhouse gas emissions, they can be utilized for distributed generation to maintain the dependability of the current system (Kumar et al., 2020).The cost of solar panels and other components has drastically decreased over the past 20 years due to technological improvements, which have also improved system efficiency and raised system yield and reliability. All of these factors have resulted in lower energy prices. This has to do with the PV module plant that has experienced the highest rise in installed capacity. Over 635 GW of photovoltaic capacity had been deployed globally (Benda & Černá, 2020). Due to importance of this energy different manufacturer companies are in competition by contributing production of solar panel.

2.9.2 Voltage and current sensor unit

Measurement and monitoring of the electrical parameters of the photovoltaic (PV) array are crucial functions of voltage and current measurement devices in an MPPT system. These blocks have a significant impact on the voltage produced by the PV array. To determine and optimize the PV system's maximum power output, it usually comprises of a voltage divider circuit or a voltage. The voltage sensor is in charge of measuring the transducer, which creates a proportionate electrical signal out of the PV array voltage.

2.9.3 PWM Generation unit

The PWM (Pulse Width Modulation) production unit in an MPPT system is in charge of producing the control signals that manage the power converter to preserve the array's maximum power extraction.

Usually, a micro-controller or a specialized PWM controller makes up the PWM generation unit. To provide the proper PWM signals, it makes use of the controller's voltage and current data. The power provided from the PV array to the load or energy storage system is determined by the switching action of the power converter, which is adjusted by the PWM signals.

Using a feedback loop, the PWM generation unit continually modifies the duty cycle in response to measured PV array voltage and current. In order to keep the system at or close to MPP, it compares the actual operating point with the peak power and modifies the duty ratio.

2.9.4 Maximum Power Point Tracking (MPPT)

MPPT is one of the applications that resulted from power electronics, which is still developing. It is essential to have a solid understanding of PV characteristics in order to comprehend and construct MPPT. It is becoming more common in off-grid of renewable energy sources as well as renewable energy tied with grid. It enhances the power obtained from a PV module or array with varied operating conditions by connecting a PV generator, load, and power electronic device.

In uniform sunlight irradiance, the PV module receives similar radiation. In this scenario, P-V characteristics curve of the module shows one peak due to the nonlinear characteristics of solar. This peak shows the maximum operating voltage of the array. Therefore, the system is expected to function at this point or close to the point to extract maximum power with help of the MPP algorithm. Conventional methods such as Perturb and observe, Hill climbing method, and Incremental conductance has been applied for to optimize the power extraction from the array. These methods work well under uniform irradiance (Bhattacharyya et al., 2021).

However, because each PV module operates at a distinct voltage, when they are exposed to non-uniform irradiance, their P-V curve characteristics show many peaks. Extracting the maximum power in this line is very challenging due to the formation of many peaks. Thus, traditional MPP algorithms are unable to collect maximum peak power in this condition. Thus, the output power can be optimized by heuristic methods such as Grey Wolf, PSO, and Genetic Algorithm. Their derivation-free processes, adaptability, and capacity to prevent local solution stagnation are the reasons for the selection heuristic method.

This thesis, therefore, selected the grey wolf algorithm as a non-conventional method and the P&O algorithm as a conventional method for maximum power extraction.

2.9.5 Boost Converter

A DC-DC boost converter is a power conversion device that is used to increase the voltage of a DC power source. It is commonly employed in numerous applications where a higher voltage level is required. It processes the step-up of an uncontrolled voltage to the higher and, stable output voltage for loads. The converter operates based on the principles of an inductor, a switch (typically a transistor), a diode, and a capacitor. It functions in two states: the on-state and the off-state. The renewable energy system can make extensive use of boost converters.

The unregulated DC voltage supplied by a solar array, which is susceptible to temperature and radiation fluctuations, serves as the input voltage for the converters under consideration.

Controlling the average DC output voltage in these converters to maintain the desired value even in the presence of variable input voltage is required. In this connection, boost converters are a power transmission medium used by solar and wind power for load injection and absorption. From an energy perspective, boost converter must continuously modify the supply of power it absorbs from the source and injects into the load in order to achieve output voltage control. The absorption and injection interval durations, which combined create a switching cycle, regulate this correction. In other way, a switching cycle is created by the converter for absorbing energy from the source and injecting it into the load. The duration of the switch on and off determines the output average voltage. Pulse width modulation switching modifies the switches on and off duration while maintaining a consistent switching frequency.

The ratio of the on duration to the switching time period is called switching duty cycle, D.

$$D=\frac{Ton}{T}, \text{ where } T=\frac{1}{fs}, \tag{2.5}$$

Depending on energy absorption and injection with relative length of switching period, converter operates in two different modes known as Discontinuous conduction mode and Continuous conduction modes (Masri & Chan, 2011).

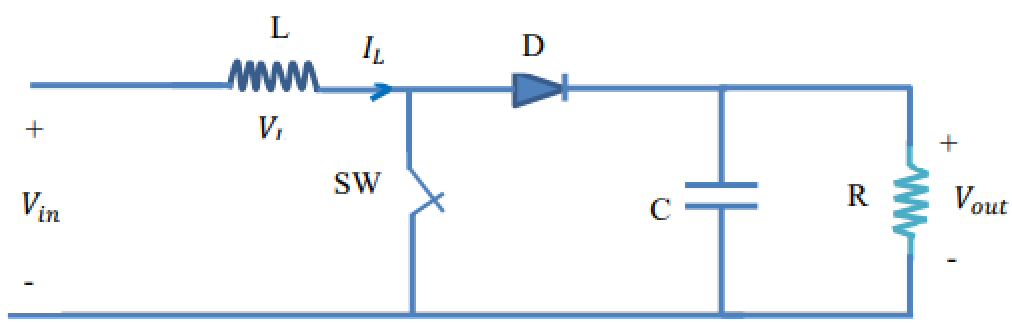

Figure 2.10 Schematic diagram of boost converter (Sai Krishna Reddy et al., 2015)

A. Continuous conduction mode

Two modes again emerged from the continuous conduction mode. As seen in Figure 2.11, mode 1 initiates when the switch is turned on at t=ton. Through inductor L and switch, the rising input current passes. Then, Inductor energy is stored. After the switch is off at t = toff, mode 2 becomes active. As indicated in Figure 2.12, the current that was passing through the switch would now pass through the inductor L, the diode, the output capacitor C, and the load

R. Inductor current decreases until the switch is turned on once more during the subsequent cycle. Energy held in the inductor element is transferred to the load. As a result, output voltage increased above input voltage and provided by;

$$Vo = \frac{1}{1-D}Vin \tag{2.6}$$

Where Vin is the input voltage, Vo is the output voltage, and D is the duty cycle

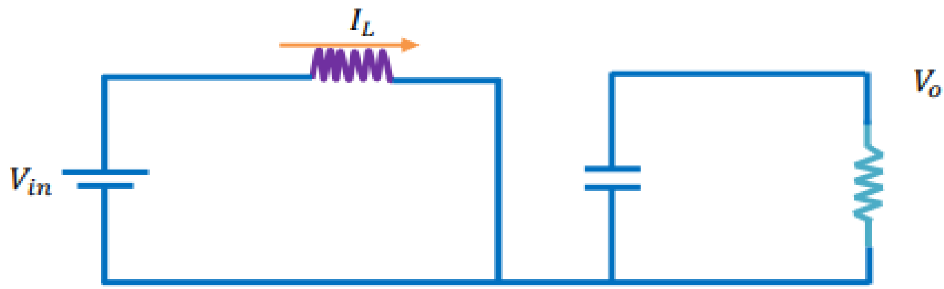

Figure 2.11 Circuit diagram for boost converter when t=ton

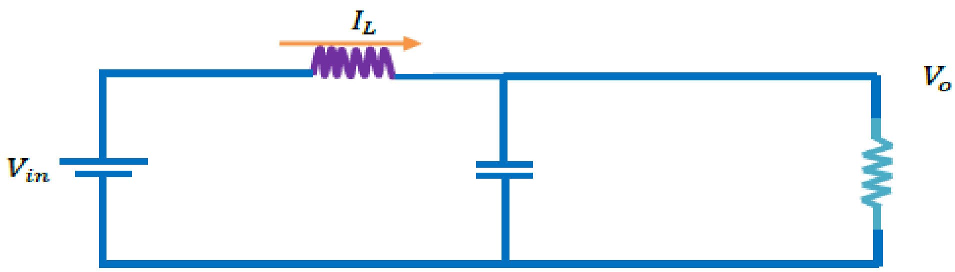

Figure 2.12 Circuit diagram for boost converter when t=off

The inductor is computed in continuous conduction mode, as shown in the Figure 2.13, so that inductor current I_L flows continuously and never zeroes out.

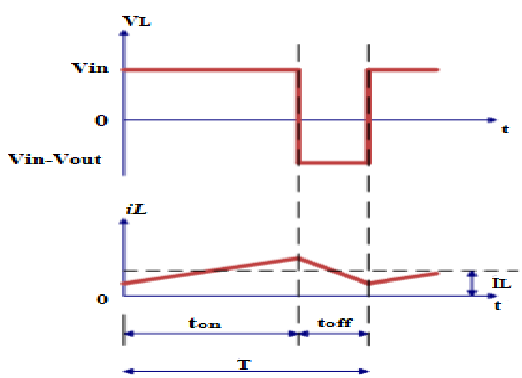

Figure 2.13 Continuous conduction mode of Boost converter waveforms (Masri & Chan, 2011)

B. Discontinuous conduction mode

Discontinuous conduction mode is an additional DC-DC boost converter operation way. The difference between two modes is caused by the Inductor current (I_L).The flow of Inductor current, I_L, is not constant. In this mode, before the switch is turned on again, there is a period of time during which the current is zero. If the chosen inductor is less than the calculated value, the converter will operate in the discontinuous conduction mode (Lan et al., 2021).

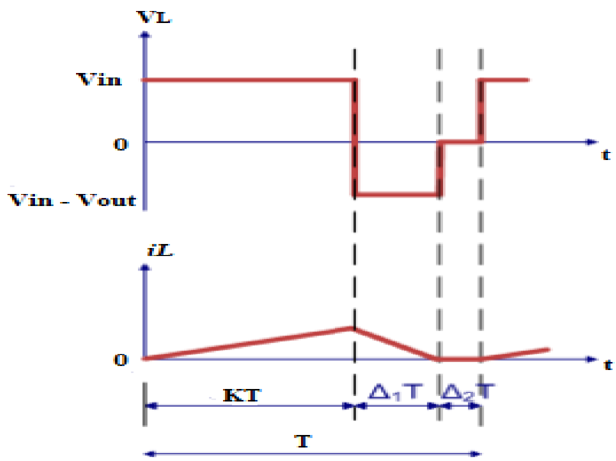

Figure 2.14 Discontinuous conduction mode of boost converter waveform (Masri & Chan, 2011)

2.9.6 DC load appliances and End uses

Nowadays, even though they run at DC, the majority of domestic appliances draw power from the AC distribution line. Accordingly, a transformer and rectifier are needed inside the appliances to convert and rectify the voltage from AC to DC. Due to these, losses are incurred throughout the conversion and repair processes. Appliances that are DC load (product) and directly linked to a DC distribution line will thereby minimize these losses. Items sold as having DC input are referred to as "DC products" in this catalogue. If the DC power input requirements of these goods were standardized, they could undoubtedly be utilized with ease in a direct-DC setting.

According to (Crowfoot, 2011), when household uses DC loads, DC system requires 22% less energy than standard AC and it is also safe for humans to touch. This section covers the appliances that have been upgraded to replace the transformer and rectifier with a DC-DC power electronics converter. The efficiency of these upgraded appliances surpasses that of conventional AC-fed equipment. Due to expansion of different energy sources, the market for DC appliances also will be high.

Based on their design and usage there are three categories of household loads

- Resistive loads
- Electronic loads
- Rotating loads

Resistive Loads: In this type of load current is converted into other forms of energy, including heat. In contrast to inductive loads, resistive loads don't produce any magnetic fields. Traditional incandescent lighting loads and the majority of electrical heaters are common examples. This kind of load draws current in proportion to the applied voltage**.** This indicates that the current and voltage are in the same phase. Electrical energy is transformed into heat by this type of electrical load. Stoves and mitad are the best examples of resistive loads.

Electronic Loads: The electronic loads in residential homes are those with internal switch mode power supple (SMPS) unit. Numerous electronic loads are utilized on a daily basis these days. Data centers, laptop computers, TVs, and security cameras are the main electronics loads that may be made energy-star or even more efficient by simply swapping out the input AC/DC converter for a buck-boost converter. They convert the AC power from an external source to DC and then adjust the voltage level. These are carried out by inefficient transformers and rectifiers, which results in inefficiency. Given that the proposed approach eliminates significant power conversion losses, the proposed DC adapter is far more efficient than the current AC adapter when fed by a DC distribution line.

Rotating Loads: This type of load includes small domestic equipment like food processors, vacuum cleaners, and mixers typically employ universal machinery. A universal machine works as well with both dc and ac power since it is constructed similarly to a series-magnetized dc machine (A. Mohamed, 2013).

2.10 PV system architecture

One of the methods to improve the tracking performance of the PV system with PSC is how the PV panels are connected to the load. Different architectures for PV system have been introduced to enhance the power processing capability and in turn the power conversion efficiency. This study employed central type of PV system architecture.

2.10.1 Central architecture

This setup uses a single MPPT controller to maximize the power output of several PV modules. In this configuration, a single boost converter processes the total power of the PV panel. Before connecting to the boost converter, all of the PV panels are connected in series or in series parallel configuration. This thesis uses this technique to reduce the complexity of control function, bulky of the system and in practical case using more than one converter requires large cost and space.

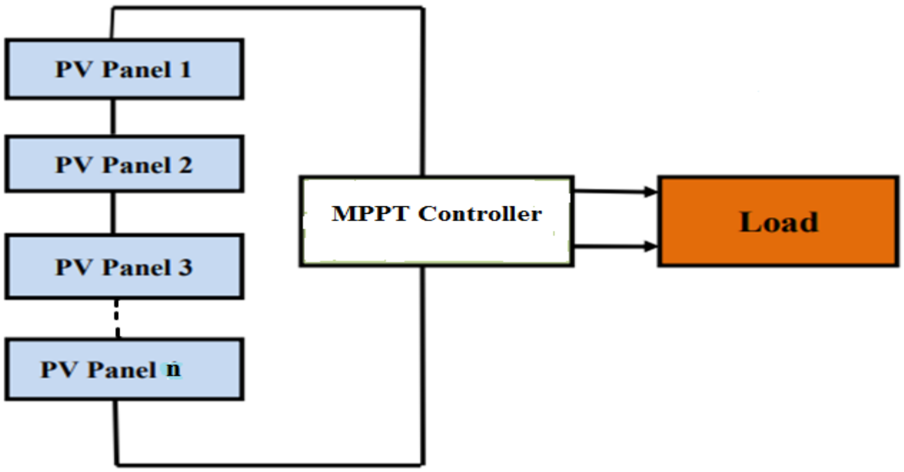

Figure 2.15 PV Configuration with Centralized MPPT controller

2.11 Review of related works

Several literature surveys have been conducted to analyze optimization techniques and architectures for photovoltaic (PV) systems.

Author in (Mohanapriya et al., 2021), the performance of solar panels was significantly improved through the implementation of a dual-axis tracking system. The research focused on developing an automated solar tracking system utilizing an Arduino prototype. The proposed system integrated an Arduino micro controller, four LDR sensors, and three stepper motors. A combination of hardware and firmware programming was employed to enable precise solar tracking. However, there were certain limitations identified in this work. Firstly, the mechanical rotation of the panel necessitated additional energy from the module. Secondly, the use of a considerable amount of materials increased complexity and cost. Lastly, the implementation of stepper motors resulted in vibrations and high energy consumption.

In (Photovoltaic, 2021), investigation and evaluation of fast and stable Constant power generation (CPG) control method across diverse environmental conditions is done. This method aims to locate the operating point to the left of the maximum power point, considering system stability. To achieve simplicity and swift response, the study employs a single diode PV equivalent model to directly estimate the MPP's location. Remarkably, the research demonstrates smooth transitioning between the maximum power point tracking (MPPT) mode and the CPG mode, unaffected by changes in irradiance, temperature, or complex real-world environmental conditions. Notably, the proposed controller eliminates the need for additional hardware such as temperature or radiation sensors. However, the paper faces challenges in terms of its complex control system implementation. Additionally, during rapid weather changes, variations around the MPPT were observed.

In (Almutairi et al., 2020), the issue of partial shading in photovoltaic (PV) systems is addressed through the utilization of a MPPT algorithm. The algorithm is implemented using the OGWO (Owl Group Optimization) method to raise collection of available energy from PV setups connected to the grid. To enhance comprehension of PV panel operation, an equivalent circuit exhibiting similar behavior is employed. The results reveal significant changes in the characteristic curves due to shading condition. A description and analysis of the complete conversion system is provided, from the PV panel to the grid connection. The gap observed from this paper is, it only focused on the partial shading of the array not on the individual module.

Author in (Nagarani & Jothiswaroopan, 2019), Proposed Performance enhancement of photovoltaic system using genetic algorithm- based maximum power point tracking. In this article, a PV system with a boost converter was mathematically modeled, and the controller's performance was examined in several environmental scenarios. This paper describes how a GA-based MPPT controller can track maximum power quickly and with less oscillation. The primary limitation of the paper lies in its failure to address the controller's ability to effectively monitor maximum power during a significant shift in both local and global optima.

Paper (Rezk et al., 2019) discussed A new statistical analysis of the global MPPT algorithms for partially shaded photovoltaic systems that utilize the majority of contemporary optimization efforts. This study explains state of the art global MPPT methods for PV systems under shading condition, which are based on contemporary optimization algorithms. It also provides a thorough statistical performance evaluation of different global MPPT algorithms under the same settings. Various statistical measures are used to assess the effectiveness of the algorithms under consideration. This comparison demonstrates that the best success rates for extracting global peaks are achieved by Grey Wolf Optimizer (GWO) and Teaching-Learning-Based Optimization (TLBO). However, this study focused only on the small range of power rating, which is convenient for power extraction.

MPPT Scheme for Solar Photovoltaic System proposed in (Haque, 2019). This study aimed to address the limitations of the traditional P&O-MPPT system when faced with higher solar irradiation and varying loading conditions. A DC-DC converter was introduced to modify the MPPT control circuit scheme, considering the load condition. The simulation study was conducted using the PSIM software to validate the proposed approach. The results demonstrate the potential of the approach to deliver efficient and accurate responses in both standalone and grid-connected photovoltaic energy conversion systems. However, it is important to note that the proposed system does not account for partial shading conditions, which can result in additional power losses.

To sum up, all of the Authors devoted their own contribution to enhance performance solar panels and optimize maximum power point tracking in PV system. The literature review reveals several gaps in the existing research. These include the reliance on mechanical sun tracking systems, the complexity of control systems associated with the CPG method, limitations in power rating coverage, and the absence of consideration for partial shading conditions. These identified gaps highlight areas that require further investigation and improvement to enhance the performance and efficiency of photovoltaic systems under partial shading condition. Therefore this thesis aims to address the aforementioned research gap by focusing on partial shading condition of PV-based residential DC microgrid as a critical factor by using Grey Wolf Optimization technique.

CHAPTER THREE

3. METHODOLOGY

3.1 Introduction

In this chapter, the focus is on the design, sizing and modeling of a photovoltaic (PV) system for a DC micro-grid. Furthermore, the development of a Maximum Power Point Tracking (MPPT) technique is examined, with the objective of obtaining the highest possible power output from the photovoltaic module in situations where partial shade occurs. The chapter also discusses the mathematical modelling of a DC-DC boost converter, which raises the voltage to match the demands of the load voltage.

Both primary and secondary sources provided data for this investigation. Primary data comprises measurements and information that are taken straight from the photovoltaic module. This includes information on temperature, irradiance, current, voltage, and output power.

On the other hand, secondary data was acquired through personal interviews, research, journals, and other relevant sources. The collected data was then analyzed. The analysis involved utilizing theoretical concepts, mathematical formulations, and modeling techniques using the MATLAB/Simulink software.

In this study GWO technique employed to track maximum power from partially shaded PV system-based DC microgrid with peak load of 4.3KW.

3.2 Description of study area

Ethiopia, located in the Horn of Africa, possesses significant solar irradiance due to its proximity to the equator and its generally sunny climate. The quantity of solar radiation received per unit area is known as solar irradiance, and it is commonly expressed in kilowatt-hours per square meter per day (kWh/m2/day).

Ethiopia's solar irradiance levels vary across the country, influenced by factors such as altitude, latitude, and local weather patterns. Generally, the northern and central regions of Ethiopia receive higher solar irradiance compared to the southern parts. Thus, using solar energy is crucial in this region of the country to boost domestic energy production, which has a significant impact on economic growth and lessens the greenhouse effect (Benti et al., 2022). Because they don't need to be converted to AC, renewable energy sources like PV systems make the construction of DC microgrids easier and more convenient (Chauhan et al., 2018).

In this study, sizing of PV system takes place depending on atmospheric condition of Sululta city to relate the result with real world and for solar energy analysis. This chapter begins with estimation of load at typical single household in this city, located in the Oromia region, with geographical coordinates of approximately 9.1853° N latitude and 38.7604° E longitude nearby Addis Ababa.

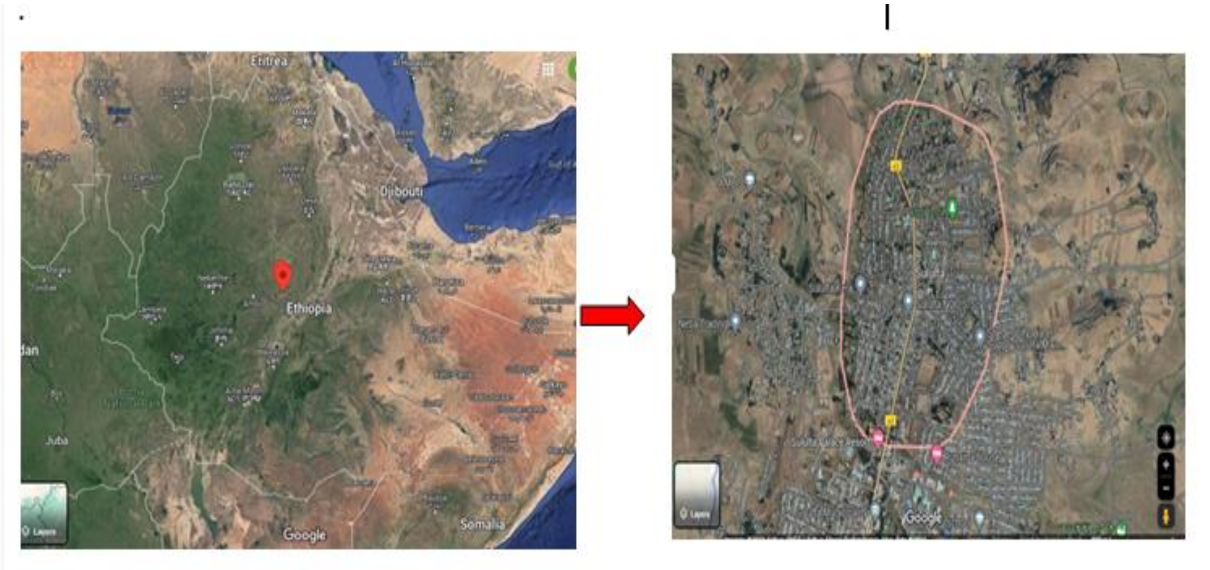

Figure 3.1 Geographical location of Sululta city (https://www.google.com/maps)

3.3 Solar Radiation Estimation

3.3.1 Orientation of PV module and mounting

In the design of any solar-powered system, the sun's location in the sky, the collecting surface's slope and orientation, and the reflective and obstructed qualities of nearby objects are the most crucial elements.

The orientations of PV modules is determined by the azimuth angle (γ) and tilt angle (β).Tilt angle β, is slope angle at which solar panels are mounted to face the sun. It is $0^0 < \beta < 90^0$) for the surface facing the equator; $90^0 < \beta < 180^0$ for the area opposite to the equator (Sado & Hassan, 2021).

Tilt angle against Horizontal needs to be equal with Latitude of PV installation site. It should be minimum angle 10-15 to prevent collection of dust and dirty of the panel.The tilt angle is typically 5–20 degrees less than the latitude in areas where the latitude is more than 30 degrees (Alayi et al., 2021).

The angle formed by the surface normal and the local longitude projected onto the horizontal plane is known as the surface azimuth angle, or γ (Kashan & Al-Qrimli, 2020).
The angular separation of sun from the local vertical is known as the zenith angle (θz). It had a direct bearing on the angle of solar elevation (Al-Qrimli& Kashan, 2020).

$$\theta z = 90-\alpha_s \tag{3.1}$$

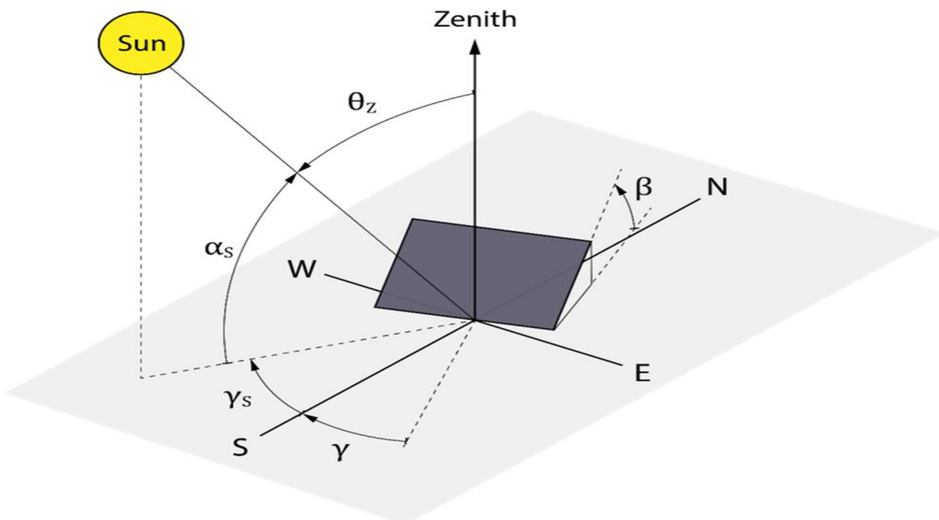

Figure 3.2 Different solar angles and mounting of PV module (Mayer & Gróf, 2020).

Two angles can be used to indicate where the solar is in the sky in relative to position on the earth: the solar azimuth angle (γs) and the solar altitude angle (α_s).
Sun beam angle to the horizontal is known as solar altitude, αs.The angle formed between the sun beam and the longitude meridian projected on the horizontal plane is known as the solar azimuth angle, γ_s. Both angles depend on the hour angle, the declination angle, and the location or latitude, ϕ (Mayer & Gróf, 2020).The next section provides their definition and their appropriate formula.

3.3.2 Analysis of solar energy

Data on radiation usually expressed as a monthly average of the daily values. The measurement of radiation is done using a pyrometer and is expressed in Mega Joules per square meter per day (MJ/m2/day) or kilowatt-hours per square meter per day (kWh/m2/day). In certain places, there is no available data on radiation; however, it can be estimated by observing the number of sunshine hours at a known site that is close to the project area.The duration of sunshine data from the adjacent station is used to analytically estimate the monthly average solar radiation using a modified version of the following angstrom equations when the irradiation data of a specific location are unknown.

$$H = H_0 \left(a + b\frac{\boldsymbol{n}}{\boldsymbol{N}}\right) \quad (3.2)$$

Whereas;

H= Average monthly radiation on a horizontal surface (MJ/m2)

H_0=Average daily monthly radiation from extraterrestrials on a horizontal surface (MJ/m2)

n=Monthly average daily of number of hours of bright sunshine

a and b are regression coefficient. It quantifies the relationship between independent variable (such as solar radiation, temperature, or panel tilt) and dependent variable (such as energy output or efficiency). It has been calculated from the relationship given by (Hailu et al., 2021);

$$a = -0.11 + 0.235\cos\phi + 0.323\left(\frac{n}{N}\right) \quad (3.3)$$

$$b = 1.449 - 0.553\cos\phi - 0.694\left(\frac{n}{N}\right) \quad (3.4)$$

Since a particular site possesses local sunshine hour data and a mean day length, these expressions are preferred.

N: The number of hours a day that can be spent in full sunshine. The following equation provides it;

$$N = \frac{2}{15}\omega_S \quad (3.5)$$

Moreover, the values of the monthly average daily extraterrestrial radiation (H_0) calculated for days giving average of each month as;

$$H_0 = \frac{24 \times 3600 \times Gsc}{\pi}\left[1 + 0.033 * \cos\left(\frac{360N}{365}\right)\right] * \left(\cos\phi\cos\delta\sin\omega_s + \frac{\pi\omega s}{180}\sin\phi\sin\delta\right) \quad (3.6)$$

Where:

G_{SC}=solar constant, 1367W/m^2

n_d=day count for the year, which begins on January 1st as 1

ϕ=latitude of the site (^{0})

δ=solar declination angle (^{0})

ω_S = An angle of the sunset hour (^{0})

Solar declination angle (δ) is the angular location of the sun south or north of the equatorial plane (Kashan & Al-Qrimli, 2020).

$\delta = 23.45 \sin\left(360\left(240 + \frac{nd}{365}\right)\right)$ (3.7)

In geometry, the term "sunset hour angel" (ω_S) refers to the position of sun with respect to an observer or a particular place on Earth at sunset. It is provided by;

$\omega_S = \cos^{-1}(-\tan^{-1}\phi \tan\delta)$ (3.8)

The average sunshine hours are the sole data that the Ethiopian Meteorological Service gathers for a few cities in the nation, and from this data that solar radiation is determined. Thus, the above-mentioned equations can be used to measure solar radiation.

The National Meteorological Service (NMS) and the National Aeronautics and Space Administration (NASA) provide the monthly average solar radiation statistics.

Accordingly, from NASA, the average monthly sun radiation of Sululta city for 2013E.C (source: https://et.freemeteo.com/weather/addis-ababa/hourly,Accessed April 2024) shown in the Table 3.1.

Table 3.1 Monthly average daily horizontal solar radiations (kWh/m2/d)

Month	J	F	M	A	M	J	J	A	S	O	N	D
Daily solar radiation Horizontal(kWh/m^2/d)	6.17	6.6	6.54	6.47	6.43	5.83	5.15	5.15	5.88	6.2	6.29	6.13

In order for a solar system to provide electricity all year round, July's minimum daily horizontal solar radiation value of 5.15 kWh/m2/d is used. The hourly irradiance fluctuation in W/m2 can be approximated using solar radiation of July and the information found in (https://et.freemeteo.com/weather/addis-ababa/hourly, Accessed April 2024). So, Table 3.2 shows hourly irradiance taken from the link.

Table 3.2 Hourly irradiance variation of 'Sululta' in W/m2

Time(hr)	00	01	02	03	04	05	06	07	08	09	10	11
Irradiance(W/m^2)	00	00	00	00	00	00	245	325	540	630	710	860
Time(hr)	12	13	14	15	16	17	18	19	20	21	22	23
Irradiance(W/m^2)	970	960	830	750	600	480	260	00	00	00	00	00

3.4 Investigation of Loads

This section completes the design of the PV system for the chosen PV module according to the power needs of standard household appliances. DC microgrid load constitutes different type of load namely, appliances with motor or rotating load, electronic load (SMPS) and resistive load as clearly described in the previous chapter.

Table 3.3 Wattages and everyday usage of DC appliances (Pfuno & Mathew, 2018).

Home appliance's	Numbers of appliances	Daily usage (hr.)	Total Wattage in(W)	Energy consumption (kWh)
Laptop	1	6	45	0.270
LED lamp	8	7	80	0.560
32 LEDTV	1	7	55	0.385
TV receiver	1	7	20	0.140
Mobile phone	3	3	18	0.540
DVD	1	3	12	0.360
Refrigerator	1	12	125	1.500
Stove	1	3	1000	3.000
Coffee grinder	1	0.5	645	0.3225
Mitad	1	3/7	3000	1.285
Total daily energy (kWh)= 8.363 Total Power (KW) = 5				

3.5 Estimation of Load

The technique of estimating how much power or electricity a certain system or device will need over a given length of time is known as load estimation. It is an essential component of energy management and has a big impact on resource allocation, grid management, and planning. A load profile in electrical engineering is a graph that shows how the electrical load changes over time. The study focuses on modeling the system initially by investigating type of load and estimating the load of power rate in a residential household's daily life.

Table 3.4 Average daily load profile

Hours	Power consumption (W)	Hours	Power Consumption (W)	Hours	Power Consumption (W)	Hr's	Power consumption(W)
00	105	06	1500	12	2200	18	2200
01	105	07	260	13	260	19	1700
02	105	08	180	14	260	20	1000
03	105	09	180	15	210	21	900
04	105	10	250	16	210	22	120
05	1200	11	4300	17	190	23	120

The overall number of appliances is used to calculate the energy demand. The maximum peak power of 4300W has been observed at 11AM from the daily load profile provided in the table.

Power designers utilize the information about energy demand, such as the maximum peak power observed and the variations in power demand throughout the day, to effectively plan and manage the electricity supply. By analyzing the data on energy consumption patterns, they can estimate how much electricity needs to be made available at different times.

For power designers to guarantee a dependable and steady power supply to satisfy consumer needs, this information is essential. By understanding the peak power requirements, they can determine the capacity of power generation and distribution systems needed to handle the maximum load. This helps in preventing power outages or system failures during periods of high demand. From Table 3.3 peak power or 4300W reached at 11AM and minimum power (105W) observed at starting from midnight to 4AM.

3.6 Design and Sizing PV system

3.6.1 PV system module

Designing and sizing a PV system involves analyzing energy requirements, assessing solar resources, selecting system configuration and sizing PV arrays. In the previous section, load estimation was discussed, focusing on analyzing the power rating of appliances and their duration of use. This analysis helps determine the energy requirements of the load and is an important step in designing and sizing a PV system. By considering the peak power ratings an accurate estimation of the total load demand can be made, ensuring that the PV system is appropriately sized to meet the energy needs.

In this work, power obtained from the PV array under partial shading conditions has been maximized based on the design of the PV system. To simulate on MATLAB/Simulink, solar module named Sun-Power SPR-X20-255 has been proposed. Table 3.5 shows electrical properties of the Sun power SPR-X20-255 solar modulus under standard test conditions (STC).

Table 3.5 Electrical characteristics of a solar module.

Sun power SPR-X20-255	
Pmax(W)	255
V_{OC}	51
Vmax(V)	42.8
Temperature coefficient of V_{OC} (%°C)	-0.24
I_{sc}(A)	6.3
Imax(A)	5.95
Temperature coefficient of Isc(%°C)	0.04
Cell per module	72
Type	Poly crystalline

Because the design of solar panel is based on mathematical formulas, theoretical calculations and standard test conditions (STC) circuit testing are required. By utilizing these theoretical values, MATLAB/SIMULINK can be used to obtain the required parameters for designing the actual circuit. The solar panel is designed and the circuit is tested in the first phase for a variety of variables, including temperature and irradiance.

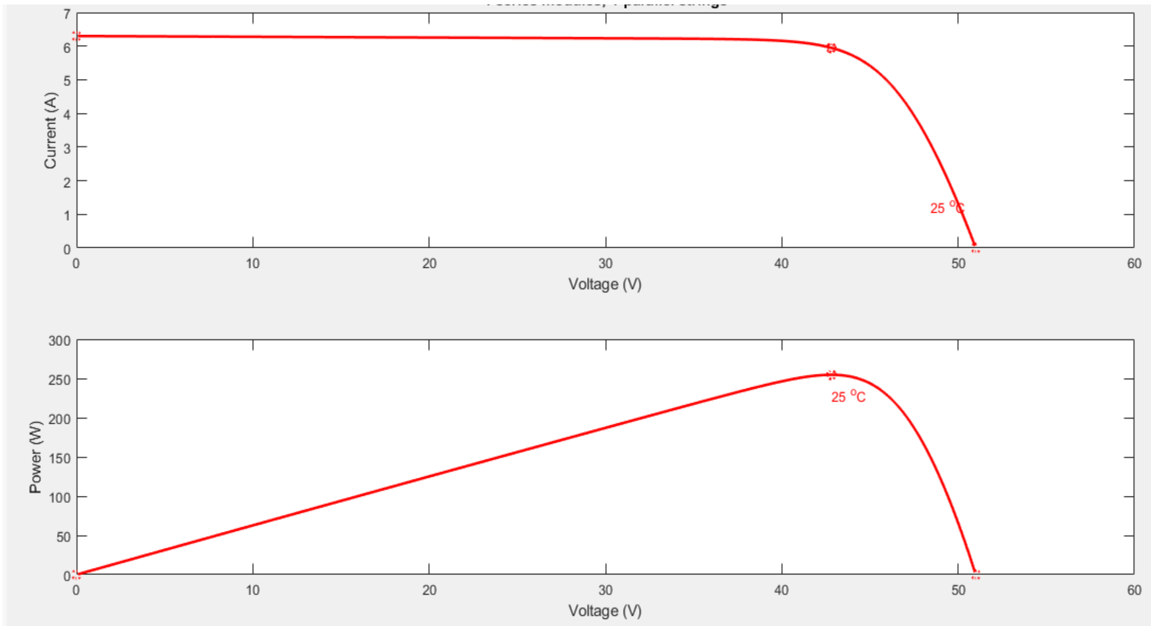

Figure 3.3 V-I and P-V characteristics at Standard Test Condition (STC).

Current-voltage (I-V) and Power-voltage (P-V) characteristics of solar panel during STC reveal important details about how well it performs. A cell temperature of 25°C, an air mass of 1.5, and an irradiance of 1000 watts per square meter are parameters used at standard conditions known as STC. At this condition P-V curve shows maximum power of the module. Under specific STC circumstances, the MPP denotes the ideal operating point at which the solar panel produces the highest production of power.

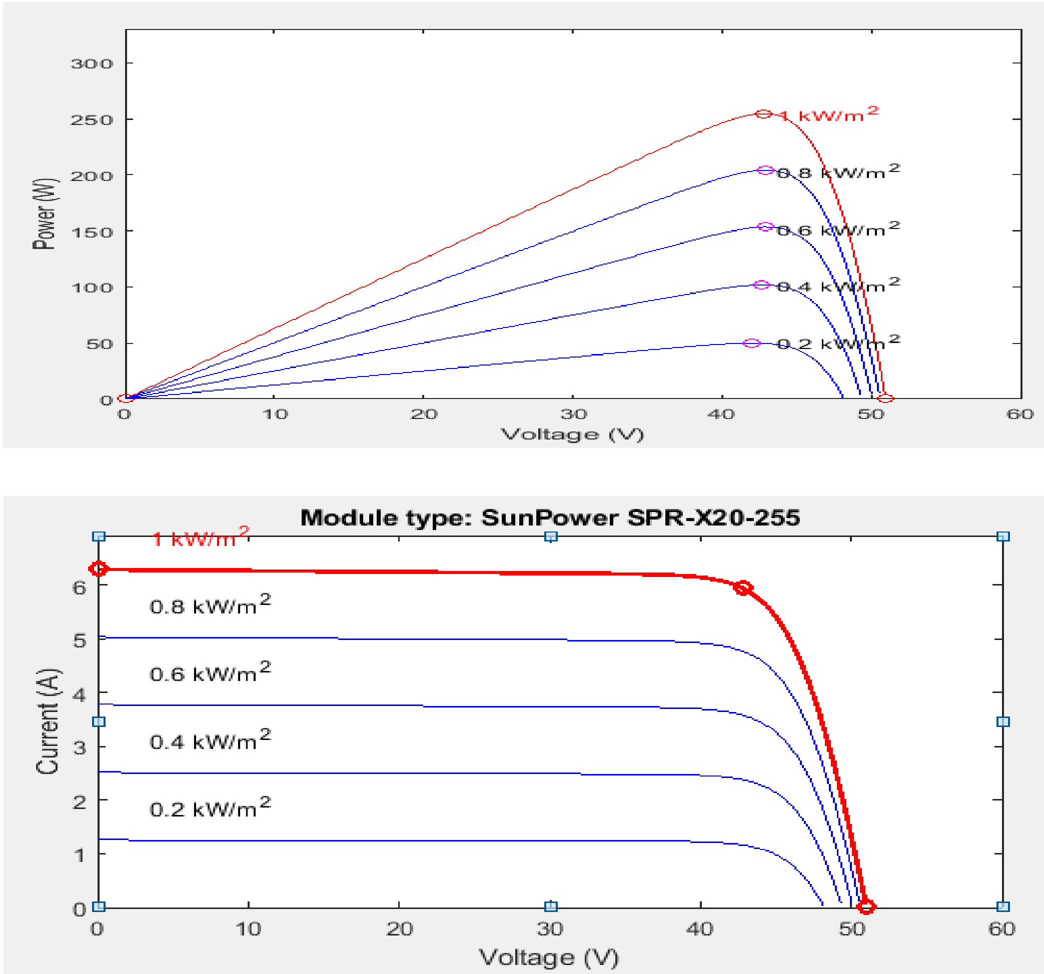

Figure 3.4 The I-V and P-V curves for different irradiance

Performance of photovoltaic devices is examined using the I-V and P-V curves at various irradiation levels. At high irradiance, the curves shift upwards, indicating increased current and power output. Under moderate irradiance, the curves show intermediate values. At low irradiance, the curves shift downwards, indicating decreased current and power output. The shape of the curves remains similar, with a knee-shaped profile representing the maximum power point (Pmax). Analyzing these curves helps optimize PV system design and evaluate solar panel efficiency in different conditions.

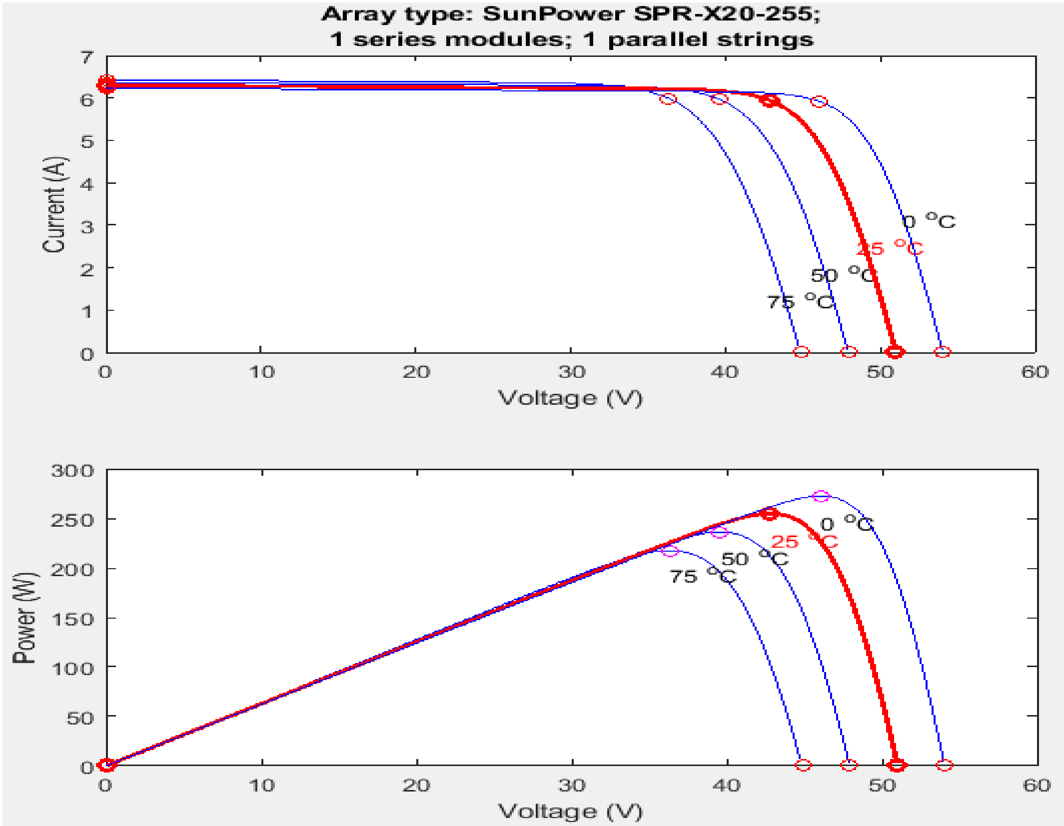

Figure 3.5 The behaviors of the I-V and P-V modules at varying temperatures.

Regardless of the amount of insolation, the current stays constant at low voltages. However, the current begins to drop as the voltage gets closer to the maximum power point. The impact of high temperature is evident in the curves, as it leads to a reduction in power output. At 75°C, for example, the maximum power voltage falls below 45V, but at 25°C, the reference temperature, the voltage can reach about 50V, leading to a higher maximum power output. At different temperatures, the I-V and P-V curves of PV modules show different behaviours.

The curves indicate that while short-circuit current (Isc) may rise at high temperatures, open-circuit voltage (Voc) decreases as a result of higher leakage current. At moderate temperatures, the curves remain relatively stable. At low temperatures, the curves show an increase in Voc and a decrease in Isc. The temperature coefficient of the module determines the extent of these variations. Understanding these behaviors is important for optimizing PV system design and evaluating module efficiency in different temperature conditions.

3.6.2 Sizing of PV system

The PV panel has been tested under different irradiances and temperature. Their I-V and P-V characteristics under standard test condition (STC) and at various irradiance levels have been clearly described. By utilizing this module, PV sizing is going to be designed to meet load requirement as follows. Determining system voltage is depends on different factors like shading conditions, available space, cost, configuration and safety condition. It is anticipated that the PV system would generate a steady voltage of 130V DC and is built to meet this load demand. Before determining required voltage from array, different voltage level has been taken and tested for sizing PV module. For instances, for < 130V the system requires around 21 modules. For >130V the system requires about 20 modules. Therefore, this lead to large space for configuration and costly for installing the PV system, as it requires large number of PV modules. Furthermore, as system requires many numbers of modules the control system of maximum power tracking also is complex and bulky. In this connection, due to large space for configurations, PV array may suffer from large partial shading condition which decreases system efficiency. Moreover, increasing voltage levels will improve the efficiency of the system. However, high voltage level will require series protection mechanism. Taking all these factors into consideration, a PV system is intended to meet this load requirement and should generate a steady voltage of 130V DC.

Module required per string;

$$Ns = \frac{\text{required Voltage}}{\text{Module Vmax}} \tag{3.9}$$

$$= \frac{130}{42.8} = 3$$

$$Imax = \frac{\text{Peak Power}}{\text{required Module Voltage}} \tag{3.10}$$

$$= \frac{4300\text{W}}{130\text{V}} = 33.77\text{A}$$

Number of string in Parallel

$$Np = \frac{\text{Load Current}}{\text{Module Imax}} \tag{3.11}$$

$$= \frac{33.77}{5.95} = 6$$

Total number of modules required = Ns ×Np = 3×6 = 18

The system uses a 3S6P configuration to meet the load. Therefore, from the above mathematical modeling, since 3 modules are a series maximum voltage of MPP is 3×42.8 =128.4V

There are 6 modules in parallel, so the maximum current of the system will be 6 ×5.95 = 35.7A

Using the aforementioned equation and following a similar process, various voltage levels were applied and tested to determine the required system voltage. The Table 3.6 presents the different voltage levels at which the tests were conducted.

Table 3.6 Different voltage levels with respective module required

Voltage level (V)	Required Module
120	21
130	18
150	20
160	20

The selection of system voltage depends on various factors. Higher voltages in PV systems can help reduce transmission and distribution losses. However, to generate high-voltage PV systems must employ large numbers of modules. This in turn leads to the requirement of large cost, space, safety considerations and bulky configuration. Generally, selecting the system voltage for a PV system is a complex decision and should be made after careful consideration of multiple factors.

3.7 Design of DC-DC boost converter

To optimize energy collection and reduce the negative effects of partial shading on the overall performance of the photovoltaic system, a boost converter's design is essential. Under these circumstances, the converter needs to be able to effectively draw power from the parts of the PV module or array that are not shaded and control the steady output voltage. To increase the voltage from the PV system to the necessary load demand, it uses a high-frequency switching technology (Can, 2019).

It constitutes a boost inductor, switching devices, Diode, Input filter capacitance, output filter capacitance and Load (H. A. Mohamed et al., 2017).All these devices and electronic circuit integrated to make the DC-DC boost converter.

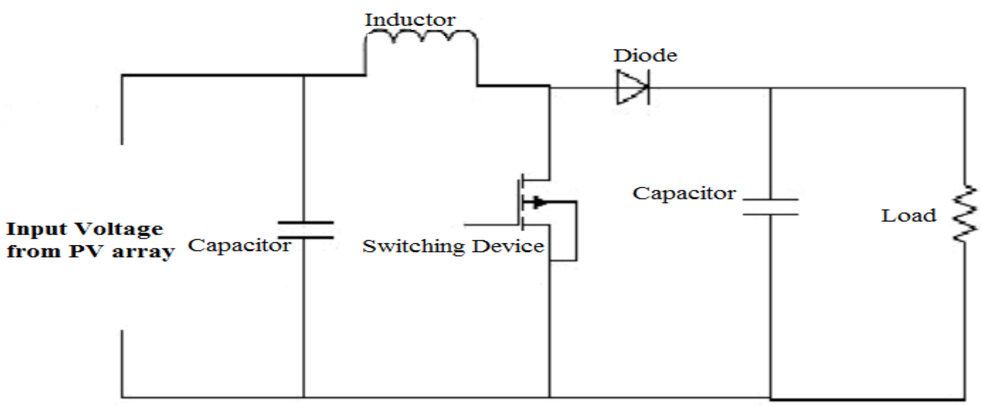

Figure 3.6 Schematic diagram for the boost Converter (Matsebele & Longe, 2020)

It connected to PV array. Due to constant variation of irradiance, input voltage to the converter is not constant or fixed. As the result, output voltage from converter gets varied and operating point of system changes. Hence, it is crucial to monitor the system's optimal performance by adjusting the converter's duty ratio. Even though, design of boost converter with PV array has no standard method to due to lack of constant input to the converter, the next section covers the design of this converter.

Two circumstances are used to determine the PV array specification: the worst condition, which has an irradiation of 50 W/m² and a temperature of 25°C, and Standard Test circumstances (STC), which have an irradiance of 1000 W/m². In this study, certain radiation levels are employed to generate power, ranging from 1000 W/m² to the worst level of 50 W/m². It is important to note that variations in irradiance primarily affect the output current of the PV array, rather than the voltage. The voltage of the PV array experiences only a ±10% change due to variations in the irradiance level (Can, 2019).

The irradiance level (W/m²) is randomly selected as input, resulting in a corresponding variation in the duty ratio within these ranges.

At 1000 W/m² and 25°C

From above design of solar panel, obtained Vmp = 130V, Imp = 33.77 and Pmp = 4300.88W

At IEC Standard of PV power, at worst condition 50W/m² and 25°C, it assumed that changing of radiation changes 9% of voltage array and 5% PV Power. So

Vmp = 0.9 × 130 = 117

Pmp = 0.05 × 4300.88 = 230W

Imp = $\frac{\text{Pmp}}{\text{Vmp}} = \frac{230}{118}$ = 1.97A

The switching frequency of converter is the rate at which the switching components in the converter circuitry turn on and off to control the output voltage. Since there are fewer switching losses at higher switching frequencies, converter efficiency is typically higher. However increased frequencies, come with increased conduction losses and switching component costs. DC-DC boost converters typically operate at switching frequencies between a few kilohertz (kHz) to several megahertz (MHz). 25Khz were chosen for switching purposes in this investigation (Thiyagarajan et al., 2014).

Defining current and voltage ripples specification also required. Small oscillations or variations in power supply's output voltage are referred to as ripple voltage. It is deviation of output voltage from the desired converter DC value due to switching action and load changes. Therefore, it is important to minimize ripple voltage to ensure stable and reliable operation of electronic systems.

In circuits or devices like DC-DC converters or AC-DC rectifiers, the term "ripple current" describes the varying or fluctuating portion of the power supply. It arises due to the switching action of the converter and the energy storage and transfer processes within the converter components. To ensure proper performance and reliability of the system, at IEC, 0.2%, 40% respectively, voltage and current ripples specifications has been arbitrarily chosen. Therefore, internal resistance of PV array at MPP and lowest power given by;

$$R = \frac{\text{Vmp}}{\text{Imp}} \tag{3.12}$$

For 1000 W/m² and 25°C

Rmp = $\frac{130}{35.7}$ = 3.64Ω

For 50 W/m² and 25°C, Rmp = $\frac{117}{1.97}$ = 60Ω

The IEC Standard for PV systems set the multiplication factor boundaries between 1 and 2.5 based on contact resistance, contaminants (impurities), and the p-n junction's depth to estimate load resistance. So, 1.3 selected to get load resistance value at lowest power.

$Ro = 1.3 \times Rmp = 1.3 \times 60\Omega = 78\Omega$

Hence, Duty ratio at MPP is given by

$$Dmax = 1 - \sqrt{\frac{Rmp}{Ro}} \quad (3.13)$$

$$= 1 - \sqrt{\frac{3.64}{78}} = 0.784$$

At 50 W/m² and 25°C, $Dmin = 1 - \sqrt{\frac{60}{78}} = 0.123$

Duty ratio needs to be varied between 0.123 and 0.784 values to maintain maximum operating voltage. Output Voltage, Vo and output current, Io of the converter at 1000 W/m² and 25°C, is given by

$$Vo = \frac{Vin}{1-D} = \quad (3.14)$$

$$= \frac{130}{1-0.784} = 600V$$

Hence Io= Vo/Ro = 600/78 = 7.69A

If solar radiance reduced to minimum smallest value of 50 W/m² and 25°C, input voltage to the converter reduced to 117V and D became 0.123 as above design. Hence, from equation (3.14) we can get

$Vo = \frac{117}{1-0.367} = 133.4$ V and Io= Vo/Ro= Io = 133.4/78 = 1.71A

The values of ripples voltage at STC will be

$\Delta Vi = 0.002 \times Vi = 0.002 \times 130 = 0.26$

$\Delta Vo = 0.002 \times Vo = 0.002 \times 600 = 1.2V$

The ripples Current of converter at highly shaded (50 W/m² and 25°C) of PV module will be

$\Delta Io = 0.4 \times Io = 0.4 \times 1.71 = 0.684A$

Input resistance (R_{IN}) at input and PV array can be determined by equation follows at 1000 W/m

$$R_i = Ro\,(1-Dmax^2) \quad (3.15)$$

$R_i = 78(1\text{-}0.784^2) = 30\Omega$

The capacitance (C) and inductor (L) of the converter can be determined by utilizing the calculated values mentioned above, using the following equation.

$$C_i = \frac{4VmpDmp}{\Delta ViRifs} \tag{3.16}$$

$$= \frac{4\times130\times0.784}{0.26\times30\times25000} = 2.1mF$$

$$C_o = \frac{2VoDmp}{\Delta VoRofs} \tag{3.17}$$

$$= \frac{2\times600\times0.784}{1.2\times78\times25000} = 402\mu F$$

$$L = \frac{VmpDmp}{2\Delta Iofs} \tag{3.18}$$

$$= \frac{117\times0.123}{2\times0.26\times25000} = 1.1mH$$

Then, the final parameter design of converter shown in Table 3.7.

Table 3.7 Specifications of boost converter

Parameters	Values	Unit
Input Voltage	117-130	V
Output Voltage	600	V
Input Capacitor	2.1	mF
Output Capacitor	402	µF
Inductor	1.1	mH
Switching Frequency	25	khz
Duty Ratio	0.1-0.8	-
Load	78	Ω

3.7.1 Switching Device

Based on its voltage and current rating, which must be greater than the maximum input voltage and current, the electronic switch, SW has been selected. According to the proposed system, the converter can handle input voltages between 117 and 130 volts and has a 4.3 KW rating. Electronic switches with the ability to handle, thyristors, MOSFETs, IGBTs, and BJTs can use as required specification to suggested design. Power IGBT has been chosen for this system (Can, 2019).

3.7.2 Diode

The output voltage limits the boost diode's reverse voltage rating. The diode conducts when the power switch is in the "OFF" position, creating a current route for the inductor to reach the output. The diode experiences its maximum peak current when the line input voltage is low and the maximum load is applied, just like in IGBTs. In addition to having the capacity to withstand the required off-state voltage stress, quick switching speeds, short reverse recovery times, and low forward voltage drops should all be taken into account when choosing a diode. The diode's ability to handle a significant amount of peak and average current is also crucial (Hasaneen & Mohammed, 2021)

3.8 GWO and Its use in MPPT

The voltage-power characteristic and the current-voltage characteristic of the photovoltaic system are non-linear and constantly change with temperature and irradiance. To follow its constant development of solar panel maximum power, MPPT control is required in the system. MPPT control activity in a photovoltaic system (PV) involves the continuous tracking of high power regardless of weather conditions and load. In this way, the maximum power of the system can be extracted. This enhances the efficiency of the overall system.

This study focuses on the extraction of maximum power tracking of a partially shaded PV module-based DC microgrid. One of the recently emerged Metaheuristic approach, the grey wolf algorithm has been selected to maximize the power extraction from PV panels which searches best operating voltage of the system. For this study, GWO has been selected due to the following reasons.

1. Simplicity; it has been inspired by very simple natural behavioral concepts.
2. Flexibility; application to various issues without requiring any unique alterations to the algorithm's structure.
3. Derivation-free mechanisms; The optimum can be found without computing the derivative of search spaces since the optimization process begins with a random solution or solutions.

4. Local optima avoidance; because of the stochastic character of meta-heuristics, which enables them to thoroughly search the whole search space and prevent stagnation in local solutions (Okwu &Tartibu, 2021).

This algorithm works with a DC-DC boost converter to directly control and adjust the duty cycle of a converter to enhance power switching. Additionally, this thesis applied the non-conventional and most common tracking method called Perturb and Observe. The description, mathematical modeling, characteristics, and flow chart development of both methods are clearly described in the next section.

3.8.1 Modeling of Grey Wolf Optimization

In 2014, Mirjalili and colleagues presented Grey Wolf Optimization (GWO), a nature-inspired metaheuristic algorithm that takes its cues from the social structure and hunting techniques of grey wolves. It is a powerful optimization technique that can be applied to various Engineering problems. In the renewable energy sector, it is crucial to optimize the amount of power extracted from photovoltaic systems that are partially shaded. The section below describes the model of the algorithm GWO and the social hierarchy and hunting mechanism of Grey Wolf.

A) Social structure of grey wolf

The social organization of grey wolves is well known; they form packs under the leadership of an alpha male and an alpha female. Within the pack, the alpha couple leads hierarchy, with the other wolves occupying subordinate roles. The algorithm was developed using the hierarchical structure and cooperative hunting behaviours of grey wolves as a basis.

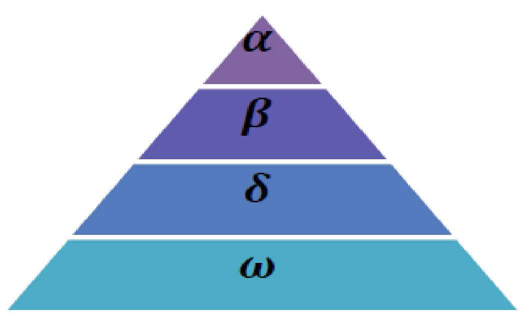

Figure 3.7 Hierarchy of grey wolf (dominance decreases from top down (Okwu & Tartibu, 2021)

Making decisions about hunting, where to sleep, when to get up, and other important issues is mostly the job of the alpha wolf. As subordinate pack members; the beta wolves support the alpha in decision-making and other pack-related tasks.

On the other hand, the delta wolves hold a position below the alphas and betas in the pack hierarchy. They assert dominance over the omega wolves and have specific responsibilities, including hunting, monitoring the pack's territory boundaries, alerting the pack to potential dangers, and taking care of sick or injured members. The omega wolves are allowed to eat their share of food because they are the lowest ranking members of the pack (Okwu & Tartibu, 2021)**.**

The following stages make up the grey wolf hunting process:

- ✓ Tracking, pursuing, and getting close to the target
- ✓ Chasing, encircling, and intimidating the target until it gives up
- ✓ Make an attack on the target

Figure 3.8 Hunting Behaviors of Grey Wolves (Okwu & Tartibu, 2021)

B. Exploration of prey

During a hunt, grey wolves will circle their prey, and the following equations simulate this behavior. The following equation can be used to predict the grey wolf's distance $\vec{D}$ from the prey.

$$\vec{D}=|\vec{C} \times \vec{X}_P(n) - \vec{x}(n)| \tag{3.19}$$

$$\vec{x}(n+1) = \vec{x}_P(n) - \vec{A}\times\vec{D} \quad (3.20)$$

Where Xp is the vector location of the prey, X is the position vector of the grey wolf, and n is shows current position. The A and C vectors are the coefficients. They give a proper balance between exploration and exploitation. A and C are determined by the following equation

$$\vec{A} = 2\vec{a}.\vec{r}1 - \vec{a} \quad (3.21)$$

$$\vec{C} = 2\vec{r}2 \quad (3.22)$$

As the iterations progress, the value of 'a' declines linearly from 2 to 0, while random vectors 'r1' and 'r2' have values between 0 and 1. By modifying the vectors A and C, the current position contributes to the optimal solution. Grey wolves can migrate to any position between their current position and the prey's position by using the random vectors 'r1' and 'r2'. The alpha, beta, and delta wolf locations in the hunting mechanism are updated using the following formulae.

$$\overrightarrow{D\alpha} = |\vec{C}_1 \times \vec{X}\alpha - \vec{X}| \quad (3.23)$$

$$\overrightarrow{D_\beta} = |\vec{C}_2 \times \vec{X}_\beta - \vec{X}| \quad (3.24)$$

$$\overrightarrow{D_\delta} = |\vec{C}_3 \times \vec{X}_\delta - \vec{X}| \quad (3.25)$$

$$\overrightarrow{X_1} = \vec{X}_\alpha - \vec{A}_1 \times \overrightarrow{D\alpha} \quad (3.26)$$

$$\overrightarrow{X_2} = \vec{X}_\beta - \vec{A}_2 \times \overrightarrow{D_\beta} \quad (3.27)$$

$$\overrightarrow{X_3} = \vec{X}_\delta - \vec{A}_3 \times \overrightarrow{D_\delta} \quad (3.28)$$

$$X_{(n+1)} = (\vec{X}_1 + \vec{X}_2 + \vec{X}_3)/3 \quad (3.29)$$

The location of the grey wolf that needs to be updated is shown by the position of X in equations 3.23–3.25. Alpha, beta, and delta wolves are located at locations Xα, Xβ, and Xδ, respectively. Depending on this, to simulate specific aspects of the hunting behavior of grey wolves when attacking prey, the vectors Dα, Dβ, and Dδ are computed in equations 3.23–3.25. The locations of the wolves in the simulation are indicated by the positions X_1, X_2, and X_3, which are calculated using vectors A and D in equations 3.26-3.28. The next location of wolves will be simulated by equation 3.29. These equations together make up the mathematical modeling technique that mimics how grey wolves hunt and attack their prey.

C. Exploitation: Prey Attack Strategies

When prey stops moving, grey wolf attacks and completes their hunt. By changing the value of vector, A, it is possible to introduce a mathematical model of the coming prey. 'A' inturn depends on the value of a. In other means, the value of A, a random value inside the interval [-a a], and ‘a’ count down from 2 to 0 during the iteration.

While vector A is populated with any values within this range, search agent will be anywhere position between its current position and next location.

Wolves generally rely on the alpha, beta, and delta positions within their pack when searching for prey. They move away from one another during the search phase and then come together to launch a coordinated attack on the prey. To mathematically represent the concept of divergence, we employ vector ‘A’ consisting of random values that exceed 1 or fall below -1. These values compel the wolf (duty) to move away from the target, ensuring a divergence in their paths. When the magnitude of vector A exceeds 1 ($|A| > 1$), it compels the search agent to move away from the current location in their pursuit of locating a potentially more suitable prey as shown figure 3.9.

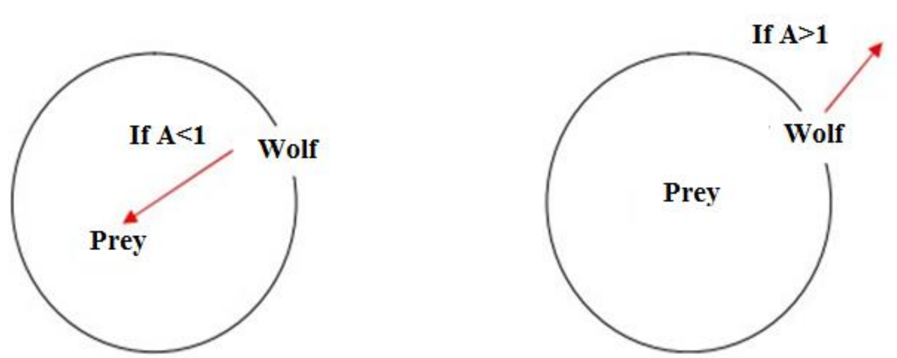

Figure 3.9 Hunting down prey and attacking prey

Vector C is an additional element of the Grey Wolf Optimization (GWO) algorithm that promotes searching phase. The vector C has random values in [0, 2], as can be observed in equation 3.22. Intentionally to ensure that vector C, it contains random values to highlight the importance of exploration throughout iterations. This particular component proves to be highly beneficial in mitigating the stagnation of local optima, particularly during the concluding stages of the optimization process. In the natural hunting environment, obstacles often prevent the wolves' way and hinder their ability to easily attack the target. This analogy aligns with the role of vector C, which simulates such obstacles and imposes similar constraints on the search agent's movement towards the prey.

The search is started with the GWO algorithm, which creates a population of grey wolves at random to represent potential solutions. The alpha, beta, and delta wolves evaluate the likely location of the prey during each iteration. The distance between each potential solution (wolf) and the prey is then updated. The parameter 'a' gradually decreases from 2 to 0, prioritizing searching phase and attacking phase, respectively. Candidate solutions end up separating from the prey when magnitude of vector A is more than 1, whereas they converge in the direction of the prey when magnitude of vector A is less than 1. The GWO algorithm comes to an end when one of the end criteria is met.

3.8.2 Problem formulation

Considering duty ratio d as the decision variable, the primary goal is to maximize the output power from the partially shaded PV array. So, the control variables are current and voltage obtained from the PV module. The algorithm optimizes the duty ratio at which maximum power can be achieved, by using current and voltage obtained from the PV array. Duty cycle D is defined as grey wolves in order to apply GWO. In this way, the formulation of the objective function is as follows.

$$P\ (d_i^k) > P\ (d_i^{k-1}) \qquad (3.30)$$

$$\text{Subjected: } d_{min} \leq d \leq d_{max} \qquad (3.31)$$

Where PV output power is represented by P, the duty ratio of the dc-dc converter is represented by d, and the lower and upper boundaries of the duty ratio are represented by d_{min} and d_{max}, which are 10% and 80%, respectively.

Several restrictions can be taken into account while utilizing the Grey Wolf Optimizer (GWO) for maximum power point tracking of a photovoltaic system. These constraints guarantee that the generated solutions (wolf) fall within the practical range of the PV system's capabilities

Voltage Limit Constraint: describes the range that should be used to restrict the voltage at the operational point.

$$Vmin \leq V \leq Vmax \qquad (3.32)$$

Where V denotes the voltage at the operating point, Vmin and Vmax represent the minimum and maximum voltage limits of the PV system.

Current Limit Constraint: describes the range that should be used to restrict the current at the operational point.

$$Imin \leq I \leq Imax \tag{3.33}$$

Where I represent the current at the operating point, Imin and Imax are minimum and maximum current limits.

Power Quality Constraint: Constraints on power quality assure that the produced power is within allowable bounds. This can be represented as:

$$P(V, I) \leq Pmax \tag{3.34}$$

Whereas P (V, I) denotes the output power at a given voltage (V) and current (I) and Pmax is required Power.

Duty Ratio Constraint: This term refers to a restriction on the duty cycle or duty ratio of a pulse-width modulation (PWM) signal, which is the ratio of the signals ON time to its overall period.

$$d_{min} \leq d \leq d_{max} \tag{3.35}$$

3.8.3 Application of GWO in MPPT of PSC PV

The P-V curve shows several peaks, including multiple local peaks (LPs) and one global peak (GP), when partial shading occurs. It is important to highlight that when the optimization algorithm identifies the maximum power point the wolves' associated coefficient vectors are getting closer to zero. The objective of the proposed system is to combine direct duty-cycle control and Grey Wolf Optimization (GWO). This means that at the maximum power point, the duty ratio became accepted value. By doing so, the system reduces a steady state disturbance that is frequently seen in conventional MPPT methods. Consequently, this reduces power loss caused by oscillations and leads to improved system efficiency.

The algorithm is typically utilized to maximize a pack's (N) positions when they hunt for a target or prey. First, it initializes the present position (X), of the wolf which is thought to be the optimal position (Pmax or Pα) for that agent. The optimization process consists of k iterations aimed at finding the optimal position for the wolf. Therefore, in the nth iteration, each wolf will have a specific position.

The position value for the (n+1) th iteration must be computed by the algorithm, and this is simulated by using equations (3.19) and (3.20)

In this study, the algorithm is utilized to increase the number of wolves (N) moving toward the objective of performing the task of maximizing power. In this sense, the objective can be defined as maximum power. D is defined as a grey wolf. Hence the method starts by giving a wolf an initial task (X) and determining where the optimal place for the wolf is alpha location. During each iteration, the duty cycle is updated, meaning that the wolf's position is changed and the iteration for searching concludes after k iterations. The flow chart of the algorithm is also given in Figure 3.10 and shows a clear explanation.

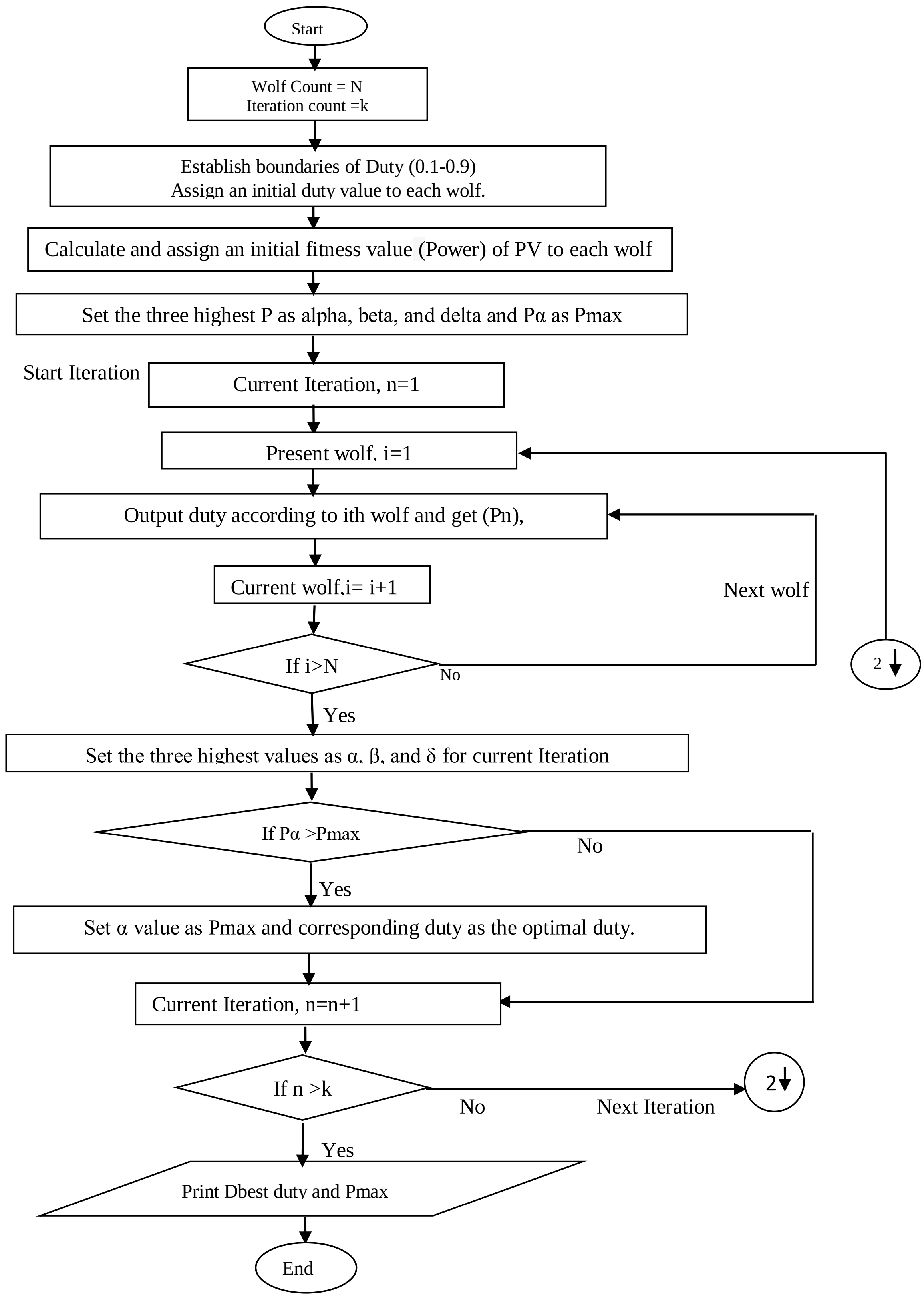

Figure 3.10 Flow chart of Grey wolf algorithm

3.8.4 P&O Method

Due to its ease of use and speedy findings under typical circumstances, P&O is one of the most popular MPPT devices and is often used as the benchmark for new MPPTs. It monitors the change in power before and after disturbances to track the MPP by varying the operating point. The controller uses the array voltages in this process to change the voltage. Initial values are assigned to these array voltages. In the first iteration, it begins with a threshold value and increases until the power starts to decrease. The disturbance will continue in the same direction that is, toward the maximum power point if the power grows. In this study, 1V perturb size was selected. In order to calculate further power, the signal unit delay blocks are utilized in this sample attenuation approach. Thus, it was determined that $\Delta P = P\mathrm{c} - P\mathrm{d}$& $\Delta V = V\mathrm{c} - V\mathrm{d}$ are calculated, where 'c' represents the original signal and d represents the delay signal.

3.8.5 P&O algorithm steps

It works by altering the PV system's operational point and tracking the ensuing shift in power output. It proceeds as follows:

1. Calculate the photovoltaic system's Output power.
2. Alter the voltage or current only a little bit to disturb the operating point.
3. Measure the new power output after the perturbation.
4. Compare the prior measurement with the new power output.
5. If the new power output is higher, continue in the same perturbation direction.
6. If the new power output is less, change the direction of perturbation.
7. Repeat steps 1 to 6 until the MPP is reached.

Limitation of the P&O method

A. Oscillation; The P&O method may exhibit oscillation around the MPP, especially under rapidly changing partial shading conditions.

B. Convergence speed; it may take longer to converge to the MPP, particularly under dynamic conditions or when the step size is too large.

C. Accuracy; it relies on local information and may not always accurately track the global MPP, especially under non-ideal conditions.

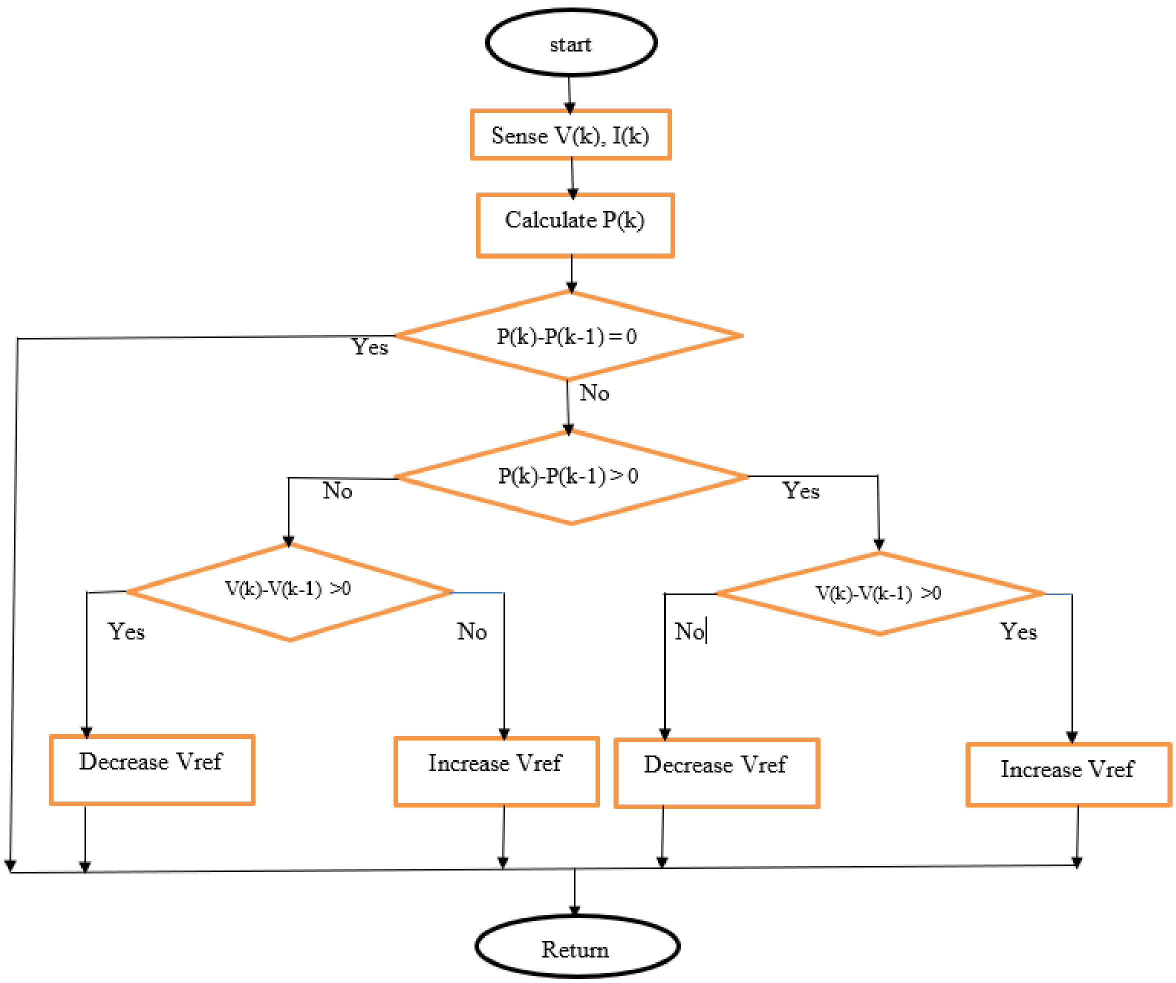

Figure 3.11 MPPT algorithm based on P&O technique

3.9 Control of Load Voltage

A boost converter is used to supply a steady output voltage to a DC resistive load when it is connected to the load. However, because the load varies continuously during the day, the load voltage might not be steady. This is particularly true when high-power appliances like mitad and stoves are attached and removed from the system. An MPPT-based boost converter in conjunction with a PI controller is utilized to maintain a steady load voltage.

Due to its inexpensive, simple design, and low structure, the PI controller is currently the most extensively used in industrial applications. Despite these benefits, the PI controller breaks down in situations when the controlled object is extremely unpredictable and nonlinear. There are two parts to the PI controller: integral and proportional parts. The supplied proportional gain, Kp, is applied to the input signal by the proportional component. The integral component amplifies the error signal by integral gain, Ki, after integrating it about time. After that, the two are combined to produce the output signal. For better performance tuning of PI parameter is important for overall efficiency.

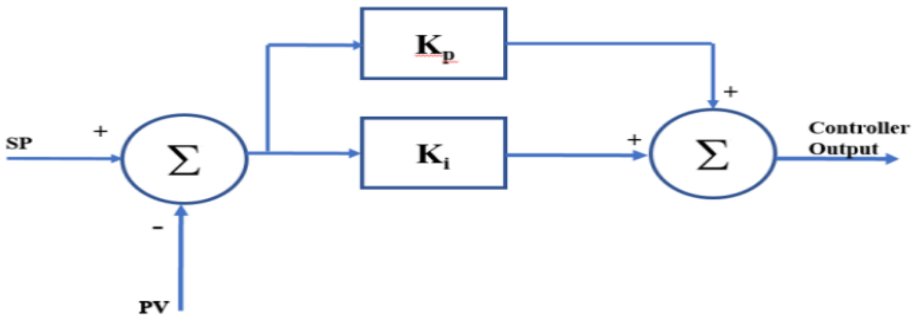

Figure 3.12 Block diagram of PI controller (Pati et al., 2023)

PI uses a voltage sensor to measure the load voltage. The difference between the reference load voltage and the measured load voltage is the error signal. After receiving the error signal, the proportional and integral terms are used by the PI controller to create a control signal. The control signal modifies the power switch of the boost converter's duty cycle, which controls the output voltage. To make sure that any fluctuations in the load voltage are adjusted, so the operation is continually repeated.

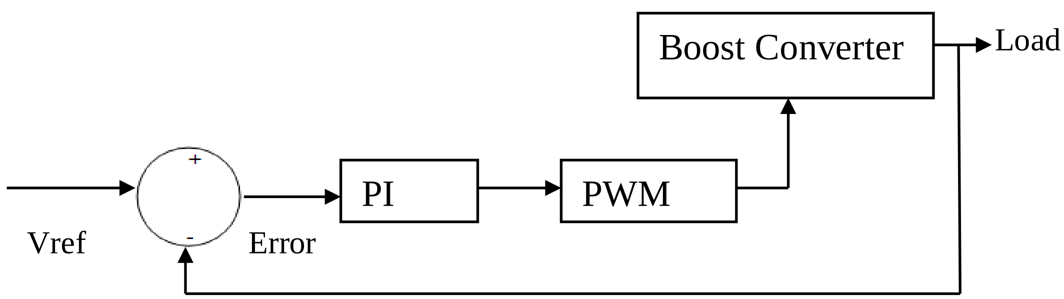

Figure 3.13 Control of load voltages with a PI and Boost converter

Since Both PI and PID controller tuning for control systems are time-consuming task, considerable effort was made at different times; the Ziegler Nichols tuned technique is widely used for calculating the parameters of both controllers. It is employed to calculate the integral gain Ki and proportional gain Kp. The integral controller Ki can be effectively utilized to eliminate steady-state inaccuracy (Yilmaz et al., 2018).

A common technique for adjusting PI is the Ziegler-Nichols (ZN) technique. In controller design, this method is frequently employed. The ultimate response method is well-known technique of Ziegler-Nichols for tuning PI controllers. It involves the following steps:

1. Set the integral gain, Ki, to zero (turn off the integral control).
2. Increase the proportional gain, Kp, until the system output oscillates with constant amplitude.
3. Measure the period of oscillation, T.
4. Calculate the ultimate gain, Ku, using the formula:

$$Ku = 4 * Kp \tag{3.36}$$

The popular equation of PI controller is given by

$$U(t) = K_p e(t) + K_i \int e(t)dt \tag{3.37}$$

Where Kp and Ki, are proportional and Integral gains and e (t) =error set point-output.

In the frequency domain, the PI output can be shown as:

$$U(s) = E(s)\left[Kp + \frac{Ki}{s}\right] \tag{3.38}$$

The provided formulas are used to calculate the values of Kp and Ki. This technique sets the integral time (Ti) to zero and the proportional times (Tp) to infinity. Then after ultimate gain is obtained it is possible to estimate initial PI setting.

Table 3.8 Tuning parameter of Z-N

Controller Type	Kp	Ki
PI	0.45Ku	0.833Pu

CHAPTER 4

4. SIMULATION RESULTS AND DISCUSSIONS

4.1 Introduction

This chapter presents an explanation of the modeling and simulation of existing systems with optimization techniques to enhance power extraction from partially shaded PV systems. The system has been modeled on MATLAB Simulink. Codes of the algorithm also have been developed in the MATLAB software's block called MATLAB Function. The simulation focuses on improving the performance of PV with a shading condition system by using the grey wolf algorithm and the Perturb and Observe method.

Eighteen PV modules (3S6P) are used in the proposed system. The existing system has been simulated under different shading conditions. In addition, the system simulated with proposed tracking techniques; the Grey Wolf algorithm, and the P&O method. As well as their tracking performance also has been discussed. Figure 4.1 shows the arrangement PV array in the system.

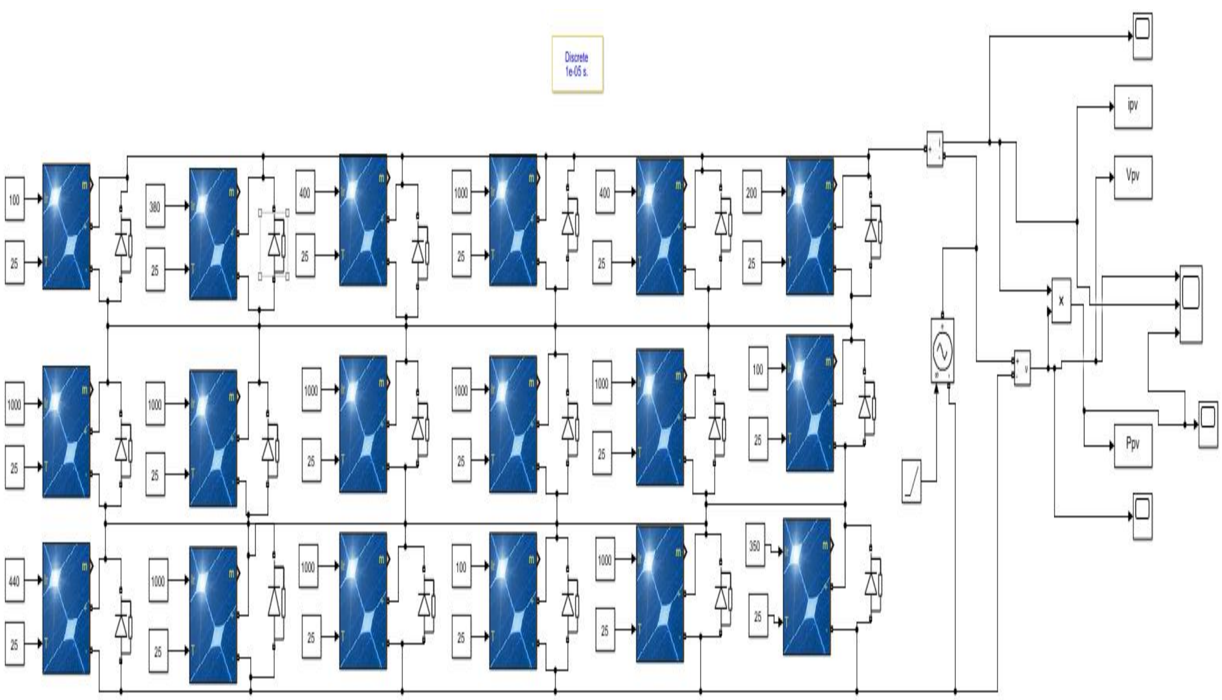

Figure 4.1 PV Array Configuration

4.2 Overall Simulink model of the system

PV system sizing and parameters of the boost converter are determined mathematically. Accordingly, to meet the load voltage, 18 PV modules are required and they receive different solar irradiances. This system consists of eighteen Sun-power SPR-X20 with 255W ratings and a DC-DC boost converter. The converter operates at 25 kHz, a filter inductance of 1.1mH, a filter Input Capacitor of 2.1mF, an output Capacitor 402mF, and 78Ω resistive load.

Figures 4.2 and 4.3 show that the Simulink diagram of system-based P&O and GWO methods. P&O MPPT uses PI controller to control the load voltage by providing appropriate switching pulses with the help of PWM to feed the converter switch. As well GWO MPPT optimizes the direct duty ratio at which optimum power is extracted. To control load voltage when the load changes over time PI controller provides a corrected switching signal to the switching devices of the converter.

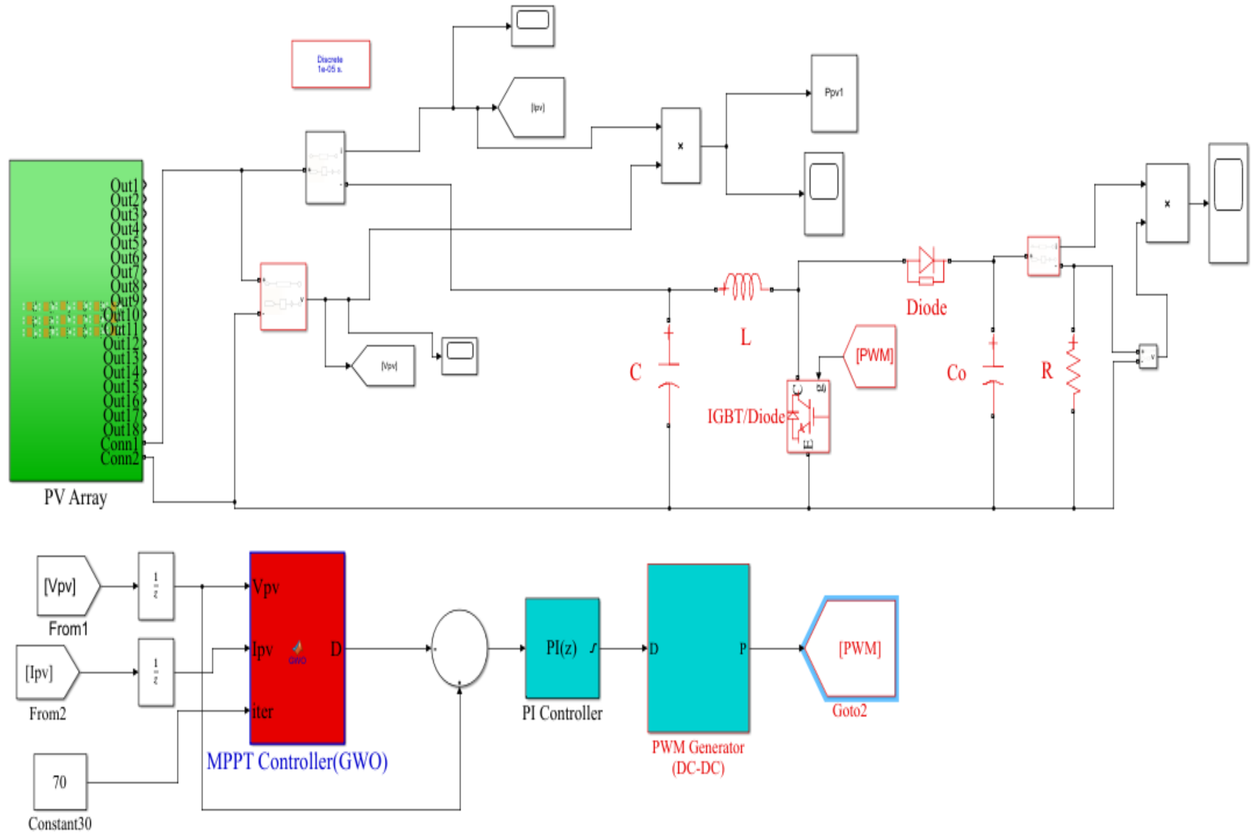

Figure 4.2 Overall proposed system with GWO

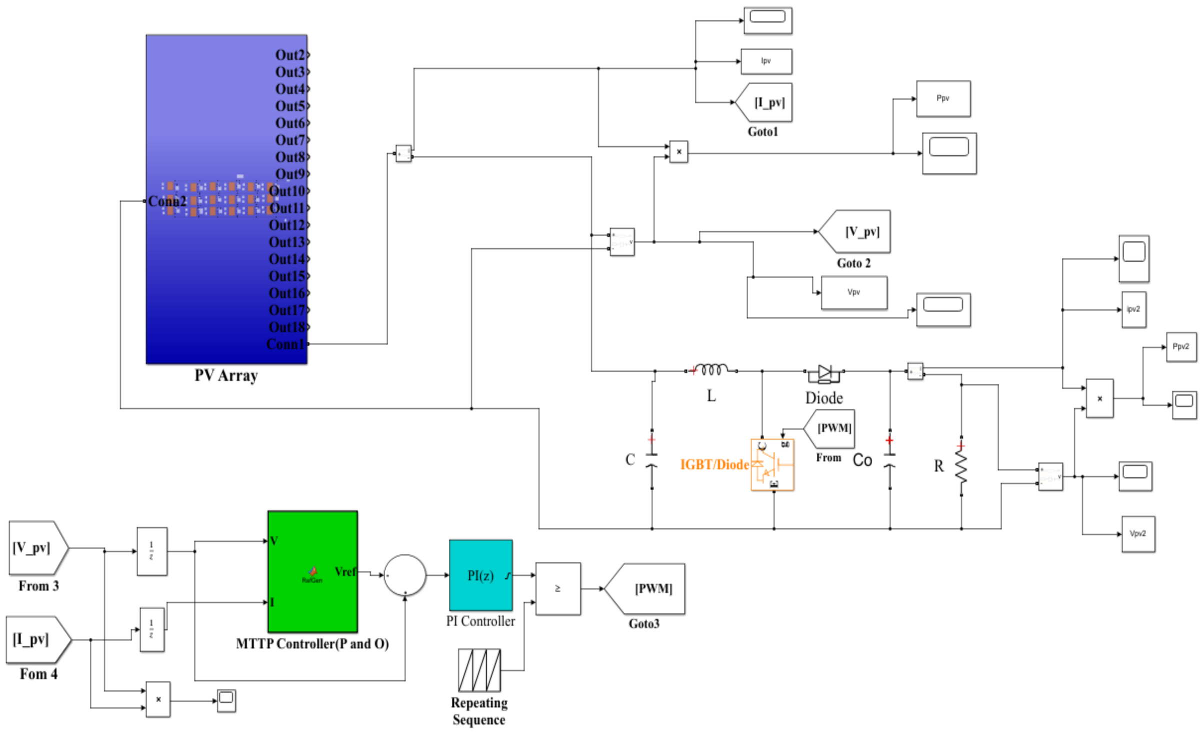

Figure 4.3 Overall proposed system with P&O

4.3 P-V and I-V Curve simulation results for different shading patterns (SPs)

The PV system is configured from Sun-power SPR-X20-255 modules in 3S6P in connections; a total of 18 modules as depicted in Figure 4.1. It measures the performance of the suggested system for various shading patterns using varying solar radiation levels. The system has been simulated for Shading Patterns 1 (SP1), Shading Patterns 2 (SP2), Shading Patterns 3 (SP3), and Shading Patterns 4 (SP4) to determine how flexible the proposed system is for non-uniform radiation reaches the PV surface. The formation of multiple peaks and P-V curves varies according to different shading patterns. Figure 4.4 indicates the result of PV generation with different cases of shading conditions (shading pattern). So, in different shading patterns the solar irradiance received by the module is different, as well as, the number of modules that receive non-uniform irradiance is also different.

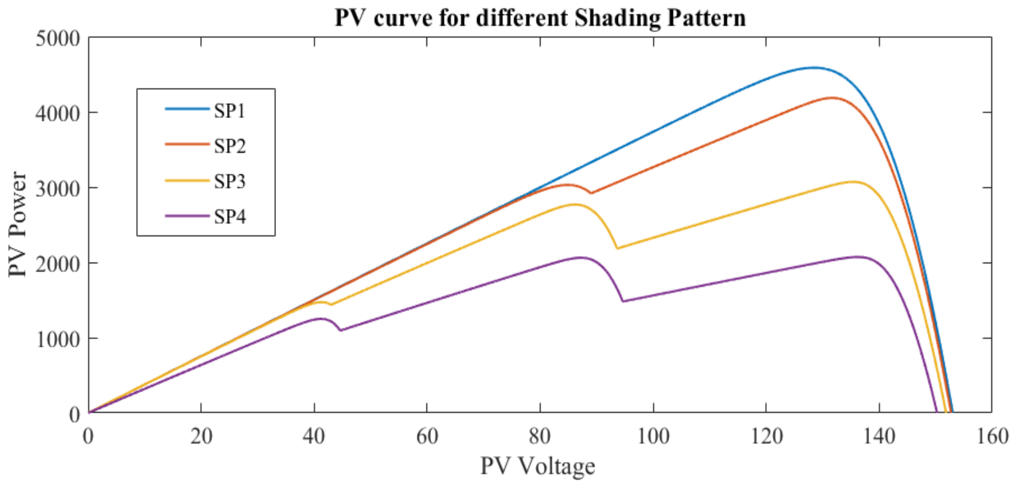

a) P-V Curve

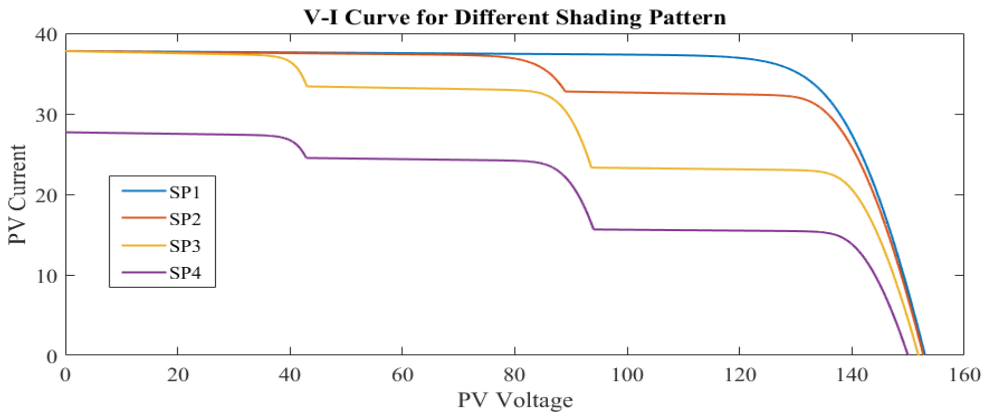

b) V-I Curve

Figure 4.4 P-V and V-I curves for various shading patterns.

As just seen from Figure 4.4a in different shading patterns, the generation capacities PV system also varies. In this connection under SP1 (or uniform solar irradiance), the system has produced a maximum power of 4300 W with one maximum peak (GMPP). The second pattern has one local peak and one global peak. With this pattern, the system has produced a maximum power of 4183W and a local peak of 3028W. The third pattern has two local peaks and one global peak. With this pattern, the system has produced a maximum power of 2277W and two local peaks of 1472W and 1400W. The Fourth pattern has two local peaks and one global peak of 2071W. The system focuses on the effect of the MPPT algorithm on the shading condition of the module. The proposed MPPT has been tracked highest peak of power with high efficiency and stable power.

Similarly, Figure 4.4b shows the generation of current versus voltage. Under different Shading patterns the amount of current generated decreases significantly. From the simulation result shown in Figure 4.4b, it is observed that variations of solar intensities highly affect the generation of current which in turn causes formation of the several peak powers in the P-V curve.

4.4 PV generation simulation results in partial shading conditions using GWO and P&O controllers

Four different random radiation levels are used to test the suggested system. Each shading pattern has a different set of solar irradiances as shown in Table 4.1.

Table 4.1 Solar irradiances of different Shading Patterns

Shading Pattern	Different solar irradiance in kW/m^2
SP1	All modules receive1
SP2	0.2,0.2 and remain modules receive 1
SP3	0.1, 0.2,0.3,0.4, and remain modules receive 1
SP4	0.1, 0.2, 0.35,0.38, 0.4,0.44 and remain modules receive 1

As shown in Figure 4.1, the proposed system uses three series and six parallel PV modules that are connected to make up a total of eighteen PV modules with different irradiances at 25°C. The system tested with resistive loads of 78Ω and 45 Ω. The experiment was carried out within 0.25s simulation time. P&O and GWO (70 number of Iteration) MPPT controllers are applied to the system and the results obtained with the proposed tracking methods have been analyzed.

4.5 PV generation results under Shading Pattern 1

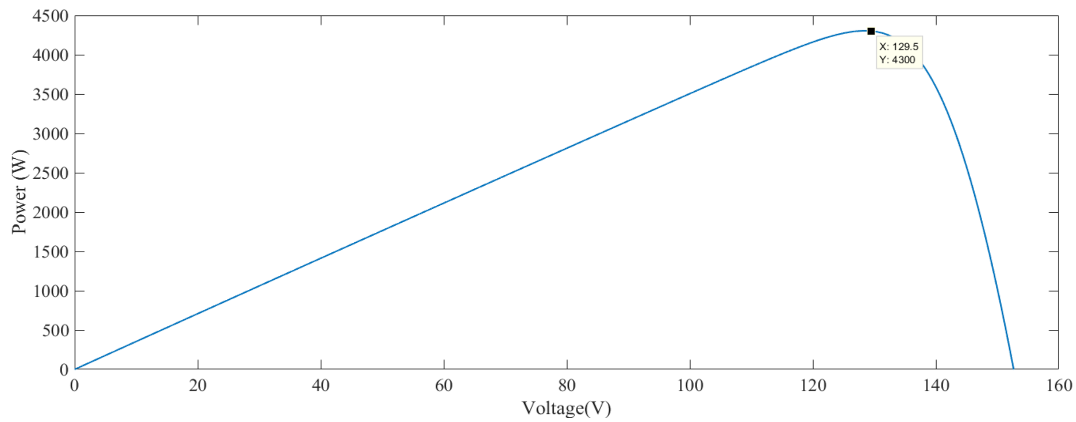

a) P-V curve under shading pattern one (SP1)

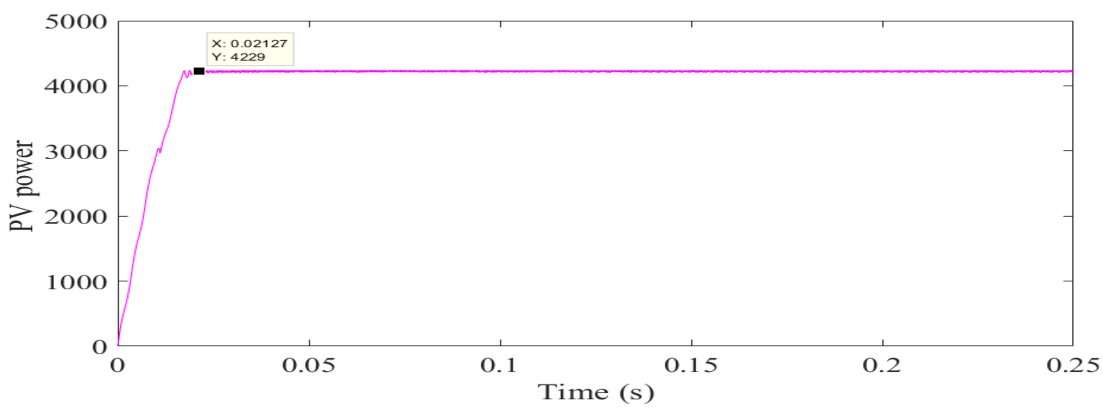

b) Simulation result of maximum power extracted by P&O MPPT

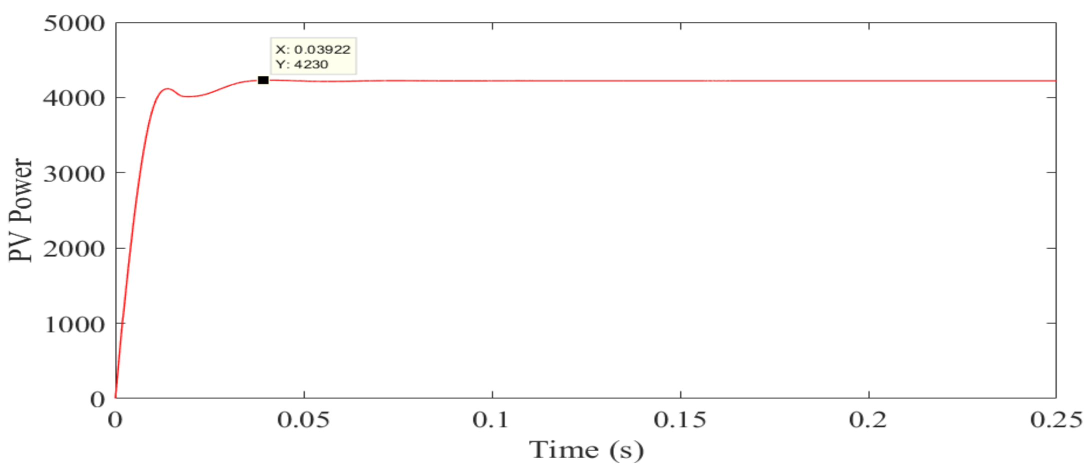

c) Simulation result of maximum power extracted by GWO MPPT

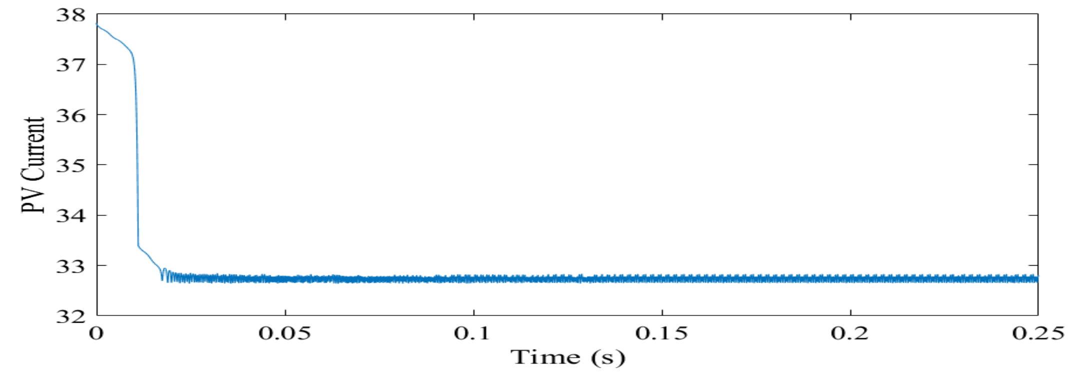

d) Current generated by PV

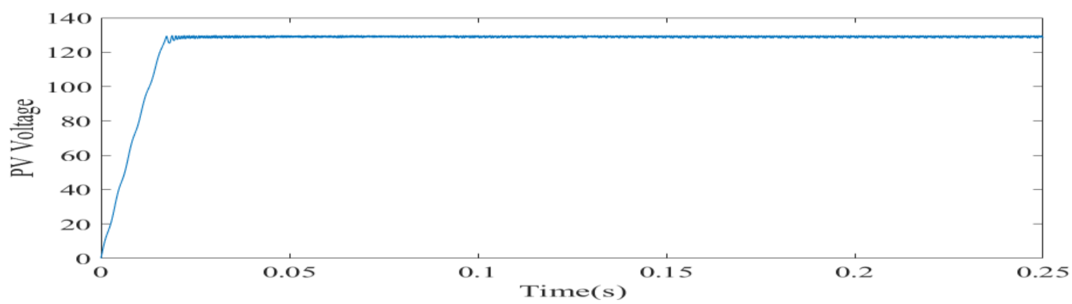

e) Voltage generated by PV

Figure 4.5 PV system power, voltage, and current during MPPT by P&O and GWO with a 78Ω load

As shown in Figure 4.5 (a) the P-V curve under shading pattern one shows only one peak with maximum power production of 4300W.Hence both algorithms are expected to collect this maximum power available from the system. Thus, as illustrated in Figure 4.5 (b), the P&O MPPT controller retrieved a maximum power of 4229W with a tracking efficiency of 98.34%, or with little power loss, and a convergence time of 0.02127s. Moreover, with 98.37% tracking efficiency, GWO MPPT was able to extract a maximum power of 4300W. i.e. with a convergence time of 0.03922s. The total amount of quantitative data confirms that the MPPT algorithms (both GWO and P&O) extract a greater amount of power from the PV. As observed from figures (b) and (c), P&O have taken a better settling time (0.02127 sec) than GWO MPPT (0.03922 sec) to extract the maximum of their power; even if; there is a small oscillation around its steady state. Even though the GWO MPPT controller extracts more power than the P&O MPPT controller, it attained MPP more slowly. This confirms that P&O MPPT also works well when the PV array is not in the condition of shading. The biggest problem for a large PV farm is that there is no way to get uniform solar light across the whole surface of the PV system because of shadows cast by structures, poles, roofs, and maybe dust on certain module surfaces.

From Figure 4.5 (d), and (e) it is observed that 128.8V and 32.9 of the PV arrays have been extracted with small oscillation. The current and voltage measured by both algorithms are almost the same. This demonstrates that P&O MPPT also extracts power well when the PV array is subjected to consistent light.

The above experiment simulated with 78Ω resistive load according to system design. The converter boosted the voltage up to 570V to meet the required load. Under uniform irradiance, if the load is reduced to 45Ω the converter supplies the appropriate voltage to the load to maintain constant power. With uniform sunlight, the system's reaction to a change in load is depicted in Figure 4.6.

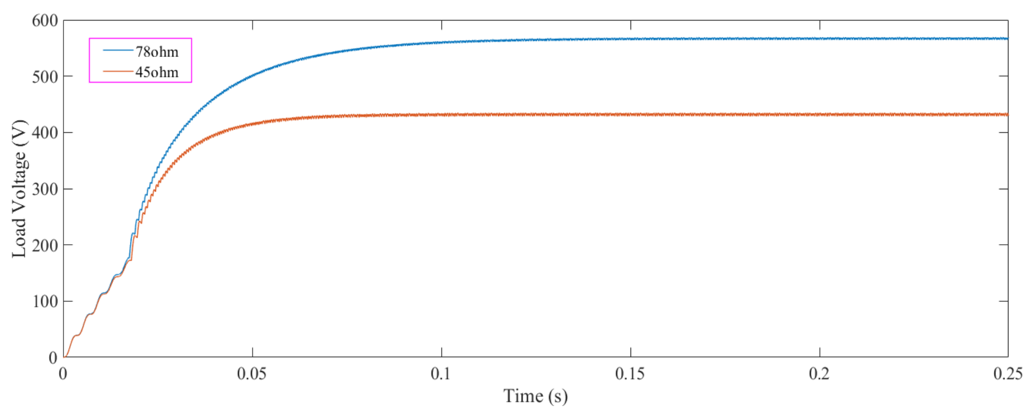

a) Load voltage

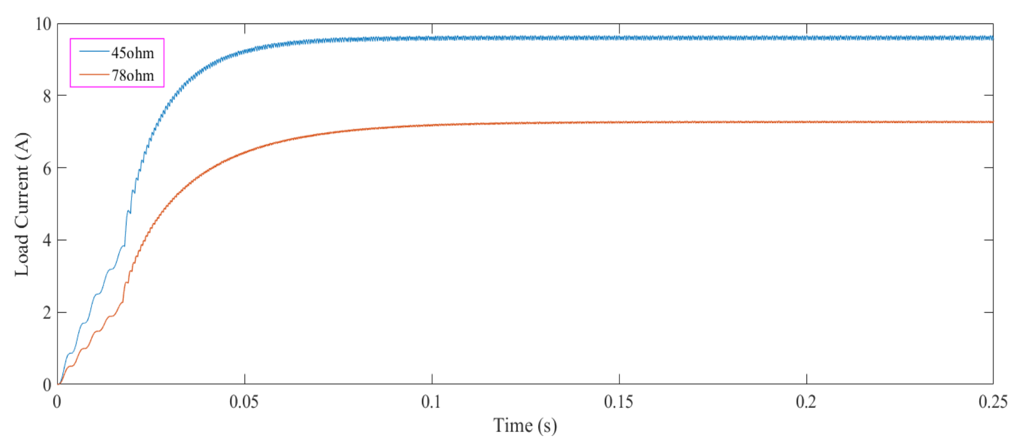

b) Load current

Figure 4.6 Voltage and current response of the proposed system with 78Ω and 45Ω.

To verify the application of the converter with load variation, the result was observed when the load changed from78Ω to 45Ω. In this line, Figure 4.6 (a) and (b) indicate the current and voltage response of the system when the load changes. At a maximum load of 78Ω, the boost converter increases voltage up to 570V with a current of 7.4A as shown in Figure 4.6 (a) and (b). However, if a load becomes 45Ω with the same uniform radiation, the MPPT controller adjusts the appropriate duty cycle fed to the converter to control load voltage with load varies. In this way, the voltage became 436V and with a load current of 9.69A to maintain a constant power of 4225W. Hence, to maximize power flow, the converter modifies the necessary load voltage and current.

In Table 4.2, all other significant PV system parameters are given in the quantitative form.

Table 4.2 Comparison of P&O and GWO performance of various parameters for shading pattern 1 (SP1)

Parameters	Result of the Shading Pattern one from MPPT Algorithms (P&O and GWO)	
	P&O	GWO
Pmax, ref (Pmpp)	4300.83W	4300.83W
Pmppt	4229W	4230W
Vmppt	127.97V	128.4V
Imppt	33.046A	32.94A
Ts	0.02127s	0.03922s
Tracking efficiency (%)	98.34	98.37
Magnitude of Oscillation	Very small around MPP	No around MPP

4.6 PV generation results under Shading Pattern 2

The schematic circuit of the PV system and overall circuit model are shown in SIMULINK Figures 4.2 and 4.3. The P-V curve under SP2 is shown in Figure 4.3a. It has one local peak of 3028W and one Global peak of 4183W. The P&O and GWO MPPT approaches were also used for the effectiveness evaluations to track the highest power under this pattern.

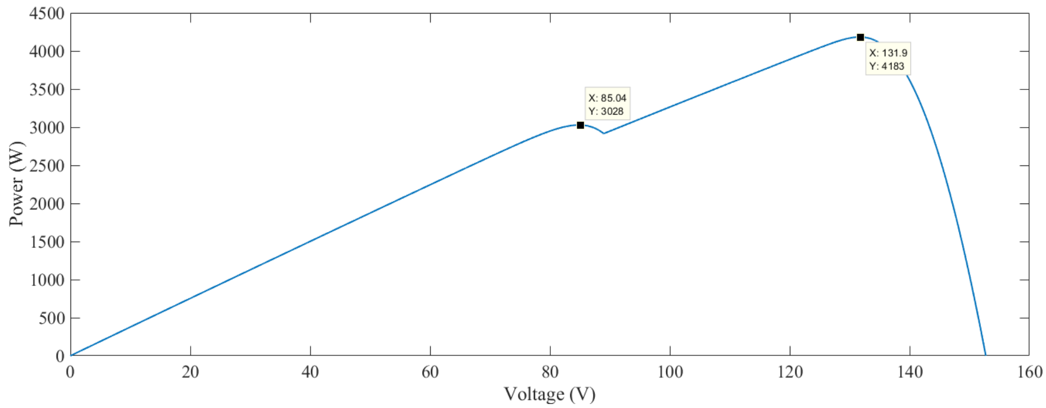

a) P-V curve under shading pattern two (SP2)

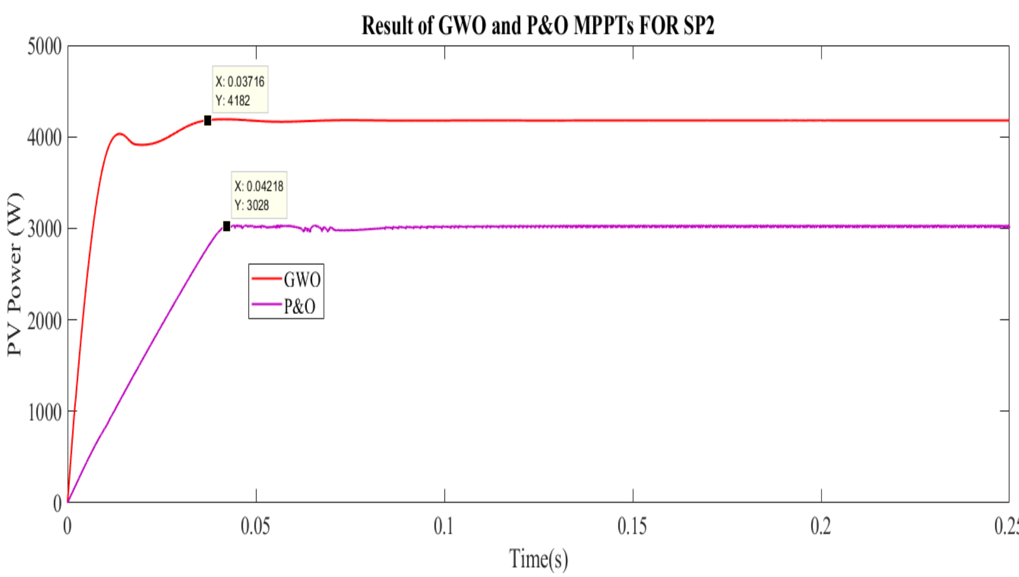

b) Simulation result of maximum power extracted by GWO and P&O MPPT

Figure 4.7 Simulation results of maximum power extraction under SP2

The P-V curve in Figure 4.7a shows that two power peaks formed in the system due to shading conditions; one local peak and one Global peak. Hence, the system is capable of producing up to 4183W of power with shading pattern two (SP2). As can be seen from the result in Figure 4.7b, the P&O MPPT algorithm was able to extract a power of 3028W with a tracking efficiency of 72.388%. In this line, P&O was able to extract the first power peak of a PV system. However, the GWO could extract the greatest power of obtained from the PV module. It extracted a power of 4182W with 99.97% tracking efficiency as shown in the Figure 4.7b. Therefore, about 27.582% (99.97-72.388) of power is enhanced by using proposed system which is not collected by conventional P&O. Enhanced power is about 1153.8W (0.27582*4183). GWO collected available power with a convergence time of 0.03716s while P&O converges at 0.04218s. The rising time MPPT with GWO is smaller than P&O; even if it indicates small harmonic oscillation at the beginning of the steady state. Additionally, it is observed that in Figure 4.7b, P&O shows oscillation at a steady state while GWO collects power without disturbances at a steady state. Consequently, compared to P&O MPPT controllers, GWO MPPT controllers are more efficient. Important parameters of both algorithms are summarized in Table 4.3.

Table 4.3 Comparison of P&O and GWO performance for Shading Pattern two (SP2)

Parameters	Result of the Shading Pattern two from MPPT Algorithms (P&O and GWO)	
	P&O	GWO
Pmax, ref (Pmpp)	4183W	4183W
Pmppt	3028W	4182W
Vmppt	85.04V	131.9V
Imppt	35.6067A	31.706A
Ts	0.04218s	0.03716s
Tracking efficiency (%)	72.388	99.97
Enhanced power	-	1153.8W (27.582%)
Magnitude of Oscillation	small around steady state	No around at steady state

4.7 PV generation results under Shading Pattern 3

The PV system again uses of similar circuit model for all patterns. There are three peaks in this pattern: two local and one global. The P&O and GWO MPPT approaches were also used for the effectiveness evaluations in order to track the highest power under this pattern.

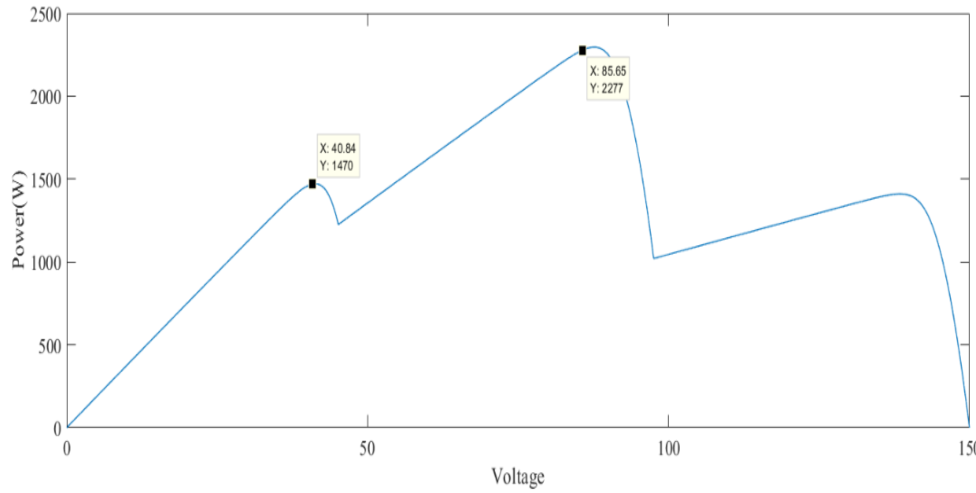

a) P- V curve under shading pattern three (SP3)

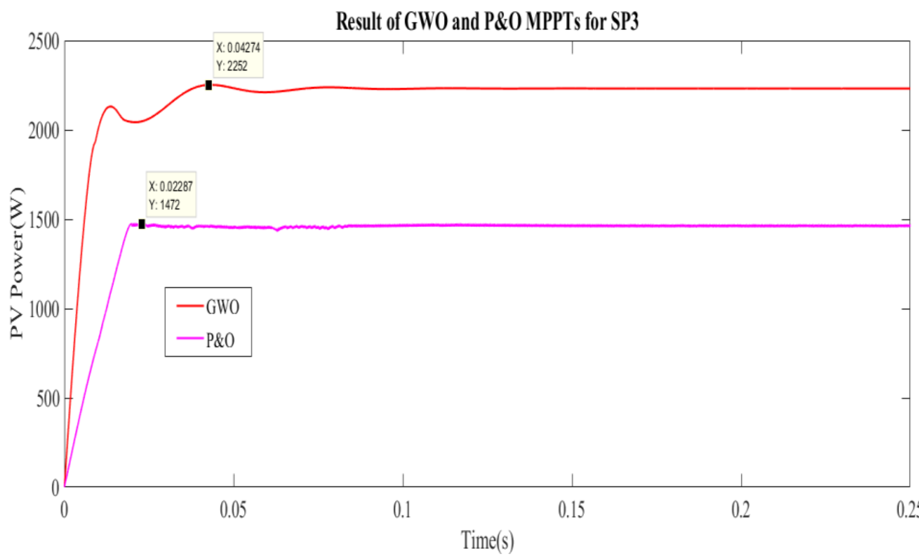

b) Simulation of maximum power extracted by GWO and P&O MPPT

Figure 4.8 Simulation results of maximum power extraction under SP3

The P-V curve in Figure 4.8a shows three power peaks formed in the system due to shading; two peaks and one global peak. Hence, the system is capable of producing up to 2277 W of power with shading pattern three (SP3). As can be seen from the result in Figure 4.8b, the P&O MPPT algorithm was able to extract a power of 1472W with a tracking efficiency of 64.64%. In this line, P&O was able to extract the first power peak of a PV system. However, the GWO could extract the greatest power of obtained from the PV module. It extracted a power of 2252W with 98.9% tracking efficiency. Therefore, about 34.26% (98.9-64.64) of power is enhanced by using a proposed system which is not collected by conventional P&O. Enhanced power is about 780.1 (0.3426*2277). GWO collected more available power with a convergence time of 0.04274s while P&O converges at 0.02287s. Additionally, it is observed that in Figure 4.8b, P&O shows oscillation at a steady state while GWO collects power with fluctuation beginning at a steady state only. However, after a small amount of time, it collected stable power from the system. Consequently, compared to P&O MPPT controllers, GWO MPPT controllers work efficiently under partial shading conditions. Important parameters of both algorithms are summarized in Table 4.4.

Table 4.4 Comparison of P&O and GWO performance for shading pattern three (SP)

Parameters	Result of the Shading Pattern three from MPPT Algorithms (P&O and GWO)	
	P&O	GWO
Pmax, ref (Pmpp)	2277W	2277W
Pmppt	1472W	2252W
Vmppt	41.36V	84.71V
Imppt	35.589A	26.585A
Ts	0.02287s	0.04274s
Tracking efficiency (%)	64.64	98.9
Enhanced power	-	780.1W (34.26%)
Magnitude of Oscillation	small around steady state	Oscillate at the beginning of convergence and stable around steady state

4.8 PV generation results under Shading Pattern 4

The PV system again uses of similar circuit model for all patterns. There are three peaks in this pattern: two local and one global. The P&O and GWO MPPT approaches were also used for the effectiveness evaluations in order to track the highest power under this pattern.

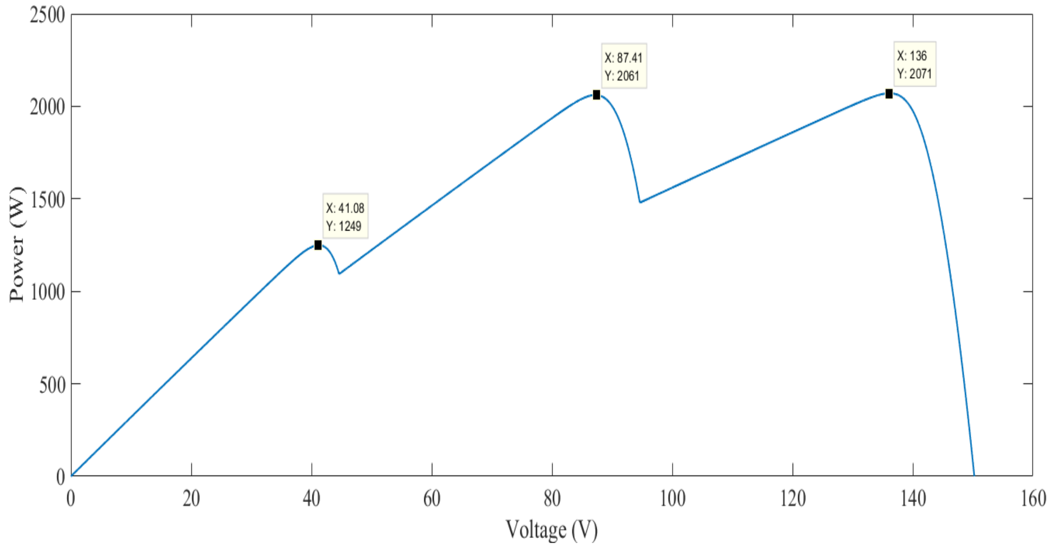

a) P-V curve with shading pattern 4 (SP4)

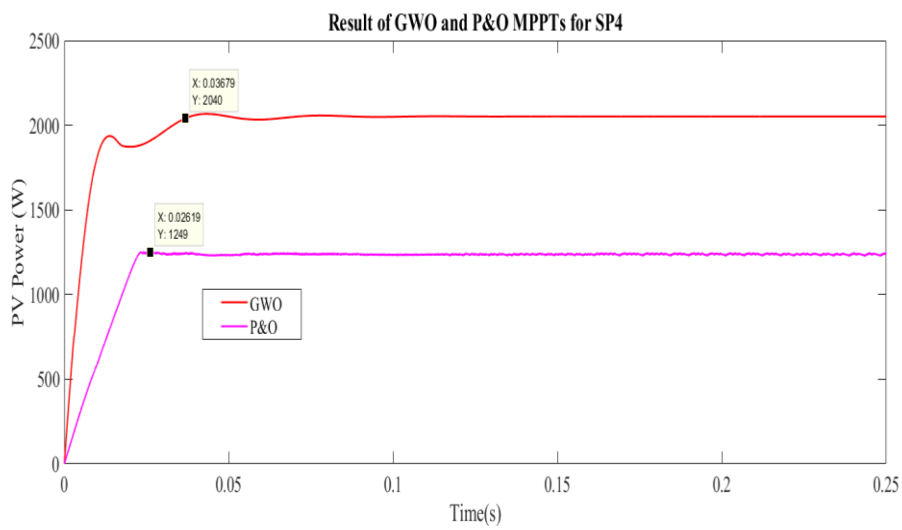

b) Simulation of maximum power extracted by GWO and P&O MPPT

Figure 4.9 Simulation results of maximum power extraction under SP4

The P-V curve in Figure 4.9a shows that three power peaks formed in the system due to shading; two local peaks and one global peak. Hence, the system is capable of producing up to 2071W of power with shading pattern four (SP4). As can be seen from the result in Figure 4.9b, the P&O MPPT algorithm was able to extract a power of 1249W with a tracking efficiency of 63.31%. In this line, P&O was able to extract the first power peak of a PV system. However, the GWO could extract the greatest power of obtained from the PV module. It extracted a power of 2040W with 98.5% tracking efficiency as shown in the Figure 4.9b. Therefore, about 35.19% (98.5-63.31) of power is enhanced by using proposed system which not collected by conventional P&O. Enhanced power is about 728.78 (0.3519*2071). GWO collected more available power with convergence time of 0.03679s while P&O converges at 0.02619s. Power trapped by GWO indicates small harmonic oscillation at the beginning of the steady state; after a very short period, it provides high stable power and tracked global peak. As it observed from Figure 4.9b, P&O tracked the first local peak with better convergence time and show oscillation at steady state while GWO collected power without disturbances at steady state. Consequently, compared to P&O MPPT controllers, under different environmental condition, GWO MPPT controller works more efficiently. Important parameters of both algorithms are summarized in table 4.5.

Table 4.5 Comparison of P&O and GWO performance for Shading Pattern four (SP4)

Parameters	Result of the Shading Pattern four from MPPT Algorithms (P&O and GWO)	
	P&O	GWO
Pmax, ref (Pmpp)	2071W	2071W
Pmppt	1249W	2040W
Vmppt	41.08V	133.96V
Imppt	30.404A	15.2205A
Ts	0.02619s	0.03679s
Tracking efficiency (%)	63.31	98.5
Enhanced Power	-	759.85W (36.69%)
Magnitude of Oscillation	Fluctuation at steady state	Oscillate at the beginning of convergence and stable around MPP

4.9 Tracking efficiency of PV system

The efficiency of the MPPT technique is a very important consideration for special PV system applications such as the power supply used in space stations and satellites. It can be determined by the following equation;

$$\eta = \frac{\text{Pmppt}}{\text{Pmax}} \times 100\% \quad (4.1)$$

Overall simulation result indicated that the proposed system has best efficiency than conventional P&O method.

4.10 Summary of Comparisons of P&O and GWO MPPT for all Shading Patterns

Table 4.6 Conclusion of performance evaluation of P&O and GWO MPPTs for varies parameters in all shading patterns of PV array.

Parameters	**SP1**		**SP2**		**SP3**		**SP4**	
	P&O	GWO	P&O	GWO	P&O	GWO	P&O	GWO
Pref	4300.83W	4300.83W	4183W	4183W	2277W	2277W	2071W	2071W
Pmppt	4229W	4230W	3028W	4182W	1472W	2252W	1249W	2040W
Vmppt	127.97V	128.4V	85.04V	131.9V	41.36V	84.71V	41.08V	133.96V
Imppt	33.046A	32.94A	35.6067A	31.706A	35.589A	26.585A	30.404A	15.2205A
Ts	0.02127s	0.03922s	0.04218s	0.03716s	0.02287s	0.04274s	0.02619s	0.03679s
Tracking Efficiency %	98.34	98.37	72.388	99.97	64.64	98.9	63.31	98.5
Magnitude of Oscillation	Very small around MPP	No around MPP	small around MPP	No around MPP	small around MPP	Oscillate at the start of convergence only	Fluctuation at steady state	Zero Fluctuation at steady state
Enhanced Power (W)		1W		1153.8W		780.1W		759.85W

CHAPTER FIVE

5. CONCLUSIONS, RECOMMENDATIONS AND FUTURE WORKS

5.1 Conclusions

Enhancement of maximum power extraction of PV-based residential DC microgrid under partial shading conditions is modeled and simulated with the Grey wolf optimization method. Simulation study results indicate that the proposed approach increases system efficiency. The proposed system was simulated on MATLAB/Simulink 2018a with different shading patterns. The system was tested with R load to confirm the efficiency of the proposed MPPT algorithm. The proposed system uses 18 PV modules with 3S6P configuration with different irradiances and at STC of temperature 25 degrees. The experiment was carried out within 0.25s simulation time. High tracking performance and low output power fluctuation are achieved by the GWO-based MPPT system rather than by the P&O-based MPPT system.

The graphs demonstrated in the fourth Chapter showed that, under partial shading conditions, the traditional controller, P&O is not able to track maximum power point among different multiple peaks. To put it another way, the outcome verifies that P&O MPPT is not flexible for varying atmospheric conditions or it only retrieves the first local maximum power point.

On the other hand, the GWO MPPT controller could extract the maximum output power or global peak of the PV system. It provides a steady output voltage that is free from oscillation–causing losses, strong tracking performance, and converges to a global power peak. This confirms that the proposed controller is adaptable to changing weather conditions, as demonstrated in the Chapter 4 results for all shading patterns.

5.2 Recommendations

Solar irradiance has a significant impact on the output electricity that a photovoltaic (PV) system harvests. A key factor in influencing the quantity of electrical energy produced is solar irradiance. Higher solar irradiance causes more photons to be absorbed by the solar cells, which raises their power production and vice versa. Furthermore, the behavior of solar cells is nonlinear, which means that there isn't a strictly proportionate relationship between the amount of solar radiation that enters the cell and the electrical current that is produced. This nonlinearity may cause the energy conversion process to possess low efficiency. To increase and harvest maximum power obtained from solar panel tracking mechanism is required. This can be done through the MPPT technique. In this thesis, the GWO algorithm is used to extract the global maximum power of the PV system under partial shade conditions. The global peak is tracked by the algorithm with small fluctuations and high convergence time.

The proposed system shows small oscillation for a short period at the start of maximum power convergence. However, better outcomes can be obtained by combining the GWO-based MPPT system with other optimization algorithms or Artificial intelligence. Tracking robustness and efficiency may be further increased by combining GWO with other metaheuristic optimization techniques.

Moreover, a resistive load simulation experiment was used in this investigation. However, the residential DC microgrid also contains another type of load like a rotating load and switching mode power supply (SMPS). But, these two loads have no block on the Matlab SIMULINK. So I can recommend to address this limitation, an effective approach is to create a time variable functioning block within the simulation. By incorporating a time variable, it is possible to design custom models to represent the behavior of rotating loads and SMPS within the DC microgrid to verify the contribution proposed algorithm under partial shading conditions.

5.3 Future Works

The study focused on the extracting of maximum power from panels under partial shading conditions during the day. Even if this problem is the dominating, there might be also other tasks that need future work.

- System can be integrated with storage battery for night time with buck-boost converter.
- Lack of standardization in selection of voltage levels is also another issue that requires future work.
- Future advancements also may include several boost converters for each series-connected module to further improve the overall efficiency of the power system.

REFERENCES

Adeeb, J., Farhan, A., & Al-Salaymeh, A. (2019). Temperature effect on performance of different solar cell technologies. *Journal of Ecological Engineering*, *20*(5), 249–254. https://doi.org/10.12911/22998993/105543

Alayi, R., Harasii, H., & Pourderogar, H. (2021). Modeling and optimization maximum power point tracking using GA for PV system. *Journal of Robotics and Control (JRC)*, *2*(1), 35–41. https://doi.org/10.18196/jrc.2149

Almutairi, A., Abo-Khalil, A. G., Sayed, K., & Albagami, N. (2020). MPPT for a PV grid-connected system to improve efficiency under partial shading conditions. *Sustainability (Switzerland)*, *12*(24), 1–18. https://doi.org/10.3390/su122410310

Benda, V., & Černá, L. (2020). PV cells and modules – State of the art, limits and trends. *Heliyon*, *6*(12). https://doi.org/10.1016/j.heliyon.2020.e05666

Benti, N. E., Aneseyee, A. B., Asfaw, A. A., Geffe, C. A., Tiruye, G. A., & Mekonnen, Y. S. (2022). Estimation of global solar radiation using sunshine-based models in Ethiopia. *Cogent Engineering*, *9*(1). https://doi.org/10.1080/23311916.2022.2114200

Bhattacharyya, S., Kumar P, D. S., Samanta, S., & Mishra, S. (2021). Steady output and fast tracking MPPT (SOFT-MPPT) for P&O and InC algorithms. *IEEE Transactions on Sustainable Energy*, *12*(1), 293–302. https://doi.org/10.1109/TSTE.2020.2991768

Can, E. (2019). The design and experimentation of the new cascaded DC-DC boost converter for renewable energy. *International Journal of Electronics*, *106*(9), 1374–1393. https://doi.org/10.1080/00207217.2019.1591529

Chauhan, R. K., Gonzalez-Longatt, F., Rajpurohit, B. S., & Singh, S. N. (2018). DC microgrid in residential buildings. *DC Distribution Systems and Microgrids*, 367–388. https://doi.org/10.1049/PBPO115E_ch15

Chen, K., Tian, S., Cheng, Y., & Bai, L. (2014). An improved MPPT controller for photovoltaic system under partial shading condition. *IEEE Transactions on Sustainable Energy*, *5*(3), 978–985. https://doi.org/10.1109/TSTE.2014.2315653

Ciocia, A., Di Leo, P., Fichera, S., Giordano, F., Malgaroli, G., & Spertino, F. (2020). A novel procedure to adjust the equivalent circuit parameters of photovoltaic modules under shading. *2020 International Symposium on Power Electronics, Electrical Drives, Automation and Motion, SPEEDAM 2020*, 711–715.

https://doi.org/10.1109/SPEEDAM48782.2020.9161878

Crowfoot, J. (2011). *Design and Modeling of the Cal Poly DC House Power Distribution System*. *June*, 111. http://digitalcommons.calpoly.edu/cgi/viewcontent.cgi?article=1548&context=theses

Dambhare, M. V., Butey, B., & Moharil, S. V. (2021). Solar photovoltaic technology: A review of different types of solar cells and its future trends. *Journal of Physics: Conference Series*, *1913*(1). https://doi.org/10.1088/1742-6596/1913/1/012053

El Hammoumi, A., Chtita, S., Motahhir, S., & El Ghzizal, A. (2022). Solar PV energy: From material to use, and the most commonly used techniques to maximize the power output of PV systems: A focus on solar trackers and floating solar panels. *Energy Reports*, *8*, 11992–12010. https://doi.org/10.1016/j.egyr.2022.09.054

Hailu, E. A., Salau, A. O., & Godebo, A. J. (2021). Assessment of solar energy potential of east Gojjam zone Ethiopia using angestrom-prescott model. *International Journal of Engineering Research in Africa*, *53*(March), 171–179. https://doi.org/10.4028/www.scientific.net/JERA.53.171

Haque, A. (2014). Maximum Power Point Tracking (MPPT) Scheme for Solar Photovoltaic System. *Energy Technology & Policy*, *1*(1), 115–122. https://doi.org/10.1080/23317000.2014.979379

Hasaneen, B. M., & Mohammed, A. A. E. (2008). Design and simulation of DC/DC boost converter. *2008 12th International Middle East Power System Conference, MEPCON 2008*, 335–340. https://doi.org/10.1109/MEPCON.2008.4562340

Heng, S. (2024). *Technology And Application Outlook of Integrated Circuits Under the Internet of Things*. *81*, 202–209.

Jamiati, M. (2021). Modeling of Maximum Solar Power Tracking by Genetic Algorithm Method. *Iranian Journal of Energy and Environment*, *12*(2), 118–124. https://doi.org/10.5829/ijee.2021.12.02.03

Kannan, N., & Vakeesan, D. (2016). Solar energy for future world: - A review. *Renewable and Sustainable Energy Reviews*, *62*, 1092–1105. https://doi.org/10.1016/j.rser.2016.05.022

Karakilic, A. N., Karafil, A., & Genc, N. (2022). Effects of Temperature and Solar Irradiation on Performance of Monocrystalline, Polycrystalline and Thin-Film Pv Panels.

International Journal on Technical and Physical Problems of Engineering, *14*(2), 254–260.

Kashan, K. A., & Al-Qrimli, F. A. M. (2020). Improving Photovoltaic Panel (PV) Efficiency via Two Axis Sun Tracking System. *Journal of Engineering*, *26*(4), 123–140. https://doi.org/10.31026/j.eng.2020.04.09

Kumar, N. M., Chopra, S. S., De Oliveira, A. K. V., Ahmed, H., Vaezi, S., Madukanya, U. E., & Castañón, J. M. (2020). Solar PV module technologies. *Photovoltaic Solar Energy Conversion: Technologies, Applications and Environmental Impacts*, 51–78. https://doi.org/10.1016/B978-0-12-819610-6.00003-X

Lan, D., Das, P., Ye, C., Sahoo, S. K., & Srinivasan, D. (2021). High-Frequency Link Matrix Rectifier in Discontinuous Conduction Mode with Reduced Input Current Distortion. *IEEE Transactions on Industrial Electronics*, *68*(7), 5517–5526. https://doi.org/10.1109/TIE.2020.2994871

Laxman, B., Annamraju, A., & Srikanth, N. V. (2021). A grey wolf optimized fuzzy logic based MPPT for shaded solar photovoltaic systems in microgrids. *International Journal of Hydrogen Energy*, *46*(18), 10653–10665. https://doi.org/10.1016/j.ijhydene.2020.12.158

Masri, S., & Chan, P. W. (2011). Design and D Converter w School of Electric 14. *Ieee*, *4*(3).

Matsebele, T. G., & Longe, O. M. (2020). Maximum Power Point Tracking with Boost Converter for Solar Laptop Charger. *2020 IEEE PES/IAS PowerAfrica, PowerAfrica 2020, December*. https://doi.org/10.1109/PowerAfrica49420.2020.9219823

Mayer, M. J., & Gróf, G. (2020). Techno-economic optimization of grid-connected, ground-mounted photovoltaic power plants by genetic algorithm based on a comprehensive mathematical model. *Solar Energy*, *202*(April 2019), 210–226. https://doi.org/10.1016/j.solener.2020.03.109

Mohamed, A. (2013). *Hybrid power system intelligent operation and protection involving distributed architectures and pulsed loads*. https://doi.org/10.25148/etd.FI13042301

Mohamed, H. A., Khattab, H. A., Mobarka, A., & Morsy, G. A. (2017). Design, control and performance analysis of DC-DC boost converter for stand-alone PV system. *2016 18th International Middle-East Power Systems Conference, MEPCON 2016 - Proceedings*, 101–106. https://doi.org/10.1109/MEPCON.2016.7836878

Mohanapriya, V., Manimegalai, V., Praveenkumar, V., & Sakthivel, P. (2021). Implementation of Dual Axis Solar Tracking System. *IOP Conference Series: Materials Science and Engineering*, *1084*(1), 012073. https://doi.org/10.1088/1757-899x/1084/1/012073

Moussa, S., Ghorbal, M. J. Ben, & Slama-Belkhodja, I. (2018). DC voltage level choice in residential remote area. *2018 9th International Renewable Energy Congress, IREC 2018*, *Irec*, 1–6. https://doi.org/10.1109/IREC.2018.8362444

Nagarani, B., & Jothiswaroopan, N. M. (2019). Performance enhancement of photovoltaic system using genetic algorithm- based maximum power point tracking. *Turkish Journal of Electrical Engineering and Computer Sciences*, *27*(4), 3015–3025. https://doi.org/10.3906/elk-1801-189

Neethu, M., & Senthilkumar, R. (2020). Comparison method of PSO and DE optimization for MPPT in PV systems under partial shading conditions. *International Energy Journal*, *20*(2), 291–298.

Okwu, M. O., & Tartibu, L. K. (2021). Grey Wolf Optimizer. *Studies in Computational Intelligence*, *927*, 43–52. https://doi.org/10.1007/978-3-030-61111-8_5

Pati, S., Pachori, N., Manik, G., & Verma, O. P. (2023). Design and optimal tuning of fraction order controller for multiple stage evaporator system. *Digital Chemical Engineering*, *9*(July), 100125. https://doi.org/10.1016/j.dche.2023.100125

Pfuno, N., & Mathew, L. (2018). *Low Voltage DC Distribution System for DC Home Appliances : A Review*. *6*(2), 455–463.

Photovoltaic, A. (2021). *High-Performance Photovoltaic Constant Power*. *57*(1), 714–729.

Rathod, K. C., Sanadi, K. R., Kamble, P. D., Kamble, G. S., Gaur, M. L., & Garadkar, K. M. (2022). Photovoltaic Solar Application Study of Cu0.5Zn0.5Se Thin Films by Chemical Bath Deposition Method. *Materials Research*, *25*(January), 0–7. https://doi.org/10.1590/1980-5373-MR-2021-0259

Rathore, N., Panwar, N. L., Yettou, F., & Gama, A. (2021). A comprehensive review of different types of solar photovoltaic cells and their applications. *International Journal of Ambient Energy*, *42*(10), 1200–1217. https://doi.org/10.1080/01430750.2019.1592774

Rezk, H., AL-Oran, M., Gomaa, M. R., Tolba, M. A., Fathy, A., Abdelkareem, M. A., Olabi, A. G., & El-Sayed, A. H. M. (2019). A novel statistical performance evaluation of most modern optimization-based global MPPT techniques for partially shaded PV system. *Renewable and Sustainable Energy Reviews*, *115*(September), 109372. https://doi.org/10.1016/j.rser.2019.109372

Righini, G. C., & Enrichi, F. (2019). Solar cells' evolution and perspectives: A short review. In *Solar Cells and Light Management: Materials, Strategies and Sustainability*. Elsevier Ltd. https://doi.org/10.1016/B978-0-08-102762-2.00001-X

Rodriguez-Diaz, E., Chen, F., Vasquez, J. C., Guerrero, J. M., Burgos, R., & Boroyevich, D. (2016). Voltage-Level Selection of Future Two-Level LVdc Distribution Grids: A Compromise between Grid Compatibiliy, Safety, and Efficiency. *IEEE Electrification Magazine*, *4*(2), 20–28. https://doi.org/10.1109/MELE.2016.2543979

Rodriguez, E., Carlos Vasquez, J., Rodriguez-Diaz, E., Savaghebi, M., Vasquez, J. C., & Guerrero, J. M. (2015). *Aalborg Universitet An Overview of Low Voltage DC Distribution Systems for Residential Applications An Overview of Low Voltage DC Distribution Systems for Residential Applications*. 318–322. http://vbn.aau.dk/files/219724154/2015_ICCE_An_Overwiew_of_LVDC_Distribution_systems_for_Residential_Applications.pdf

Sabry, A. H., Shallal, A. H., Hameed, H. S., & Ker, P. J. (2020). Compatibility of household appliances with DC microgrid for PV systems. *Heliyon*, *6*(12), e05699. https://doi.org/10.1016/j.heliyon.2020.e05699

Sado, K. A., & Hassan, L. H. (2021). *DigitalCommons @ University of Nebraska - Lincoln Photovoltaic panels tilt angle optimization Photovoltaic optimization panels tilt angle*.

Sai Krishna Reddy, M., Kalyani, C., Uthra, M., & Elangovan, D. (2015). A small signal analysis of DC-DC boost converter. *Indian Journal of Science and Technology*, *8*(January), 1–6. https://doi.org/10.17485/ijst/2015/v8is2/57787

Sara, I. D., & Faulianur, R. (2019). Grey wolf optimization for track maximum power of photovoltaic system in multiple peak power characteristics. *IOP Conference Series: Materials Science and Engineering*, *523*(1). https://doi.org/10.1088/1757-899X/523/1/012047

Suhardi, D., Syafaah, L., Irfan, M., Yusuf, M., Effendy, M., & Pakaya, I. (2019). Improvement of maximum power point tracking (MPPT) efficiency using grey Wolf optimization (GWO) algorithm in photovoltaic (PV) system. *IOP Conference Series: Materials*

Science and Engineering, *674*(1). https://doi.org/10.1088/1757-899X/674/1/012038

Thiyagarajan, A., Praveen Kumar, S. G., & Nandini, A. (2014). Analysis and comparison of conventional and interleaved DC/DC boost converter. *2nd International Conference on Current Trends in Engineering and Technology, ICCTET 2014*, *38*(0), 198–205. https://doi.org/10.1109/ICCTET.2014.6966287

Tzikas, C., Gómez, G., Donker, M. van den, Bakker, K., Smets, A. H. M., & Folkerts, W. (2017). Do thin film pv modules offer an advantage under partial shading conditions? *33rd European Photovoltaic Solar Energy Conference and Exhibition*, *November*, 1593–1596.

Windarko, N. A., Habibi, M. N., Sumantri, B., Prasetyono, E., Efendi, M. Z., & Taufik. (2021). A new mppt algorithm for photovoltaic power generation under uniform and partial shading conditions. *Energies*, *14*(2), 1–22. https://doi.org/10.3390/en14020483

Yilmaz, U., Kircay, A., & Borekci, S. (2018). PV system fuzzy logic MPPT method and PI control as a charge controller. *Renewable and Sustainable Energy Reviews*, *81*(April 2016), 994–1001. https://doi.org/10.1016/j.rser.2017.08.048

APPENDICES

Appendix A: Table 2.1: Data from NMS on Sululta's solar radiation in KWh/m2/day

Year	J	F	M	A	M	J	J	A	S	O	N	D
2010	-	-	6.64	6.09	6.12	6.22	5.13	5.17	6.46	6.45	5.99	5.88
2011	5.18	6.91	6.60	6.12	6.05	5.25	4.56	5.59	5.85	6.13	6.00	6.34
2012	6.08	6.81	6.20	6.70	6.12	5.47	5.01	-	-	6.33	6.15	6.14
2013	6.12	6.85	6.11	6.01	5.99	5.14	5.33	5.04	5.20	6.21	6.34	6.10
2014	6.02	6.87	6.73	6.03	6.13	6.05	5.25	5.68	5.33	6.04	6.33	6.07
Monthly average	**6.1**	**6.86**	**6.5**	**6.19**	**6.08**	**5.62**	**5.05**	**5.37**	**5.71**	**6.23**	**6.16**	**6.11**

Appendix B: P&O algorithm based MPPT

```
functionVref = RefGen(V,I)
Vrefmax=130;
Vrefmin=100;
Vrefinit=130;
deltaVref=1;
persistent Vold Pold Vrefold
datatype='double';
ifisempty(Vold)
    Vold=0;
    Pold=0;
Vrefold=Vrefinit;
end
P=V*I;
dv=V-Vold;
dp=P-Pold;
ifdp~=0
ifdp<0
if dv<0
Vref=Vrefold+deltaVref;
else
Vref=Vrefold-deltaVref;
end
else
if dv<0
Vref=Vrefold-deltaVref;
else
Vref=Vrefold+deltaVref;
end
end
else
Vref=Vrefold;
end
ifVref>=Vrefmax | Vref<=Vrefmin
Vref=Vrefold;
end
Vrefold=Vref;
Vold=V;
Pold=P;
```

Appendix C: Sample of GWO algorithm based MPPT

```
function D = GWO(Vpv,Ipv,iter)
%#codegen
persistent u;
persistentdcurrent;
persistent p pc;
persistent dc dcheck;
persistentdbestdworst;
persistent counter iteration;
persistentiworst;
persistentdeltad;
persistentFk;
persistent En alpha beta_posdelta_posalpha_posbeta_scoredelta_score;
if(isempty(alpha))
    alpha=0;
end
if(isempty(beta_pos))
alpha_pos= zeros(1, 1);
beta_pos= zeros(1, 1);
delta_pos= zeros(1, 1);
beta_score=0;
delta_score =0;
end
if(isempty(iteration))
iteration=0;
end
if(isempty(counter))
    counter=0;
end
if(isempty(dcurrent))
dcurrent=0.5;
end
if(isempty(iworst))
iworst=0;
dworst=0;
end
if(isempty(deltad))
deltad=zeros(4,1);
end
if(isempty(Fk))
Fk=zeros(4,1);
end
if(isempty(En))
    En=zeros(4,1);
end
if(isempty(dbest))
```

```
dbest=0;
   best=0;
end
if(isempty(p))
   p=zeros(4,1);
   pc=zeros(3,1);

end
if(isempty(u))
   u=0;
end
if(isempty(dc))
   dc=zeros(4,1);
dcheck=zeros(3,1);
dc(1)=0.16;
dc(2)=0.34;
dc(3)=0.51;
dc(4)=0.71;
end
if(counter>=1 && counter<200)
if(u>=1 && u<=4)
     p(u)=Vpv*Ipv;
end
 D=dcurrent;
   counter=counter+1;
return;
end
counter=0;
u=u+1;
if(u==6)
   u=1;
end

if(u==1)
   D=dc(u);
dcurrent=D;
   counter=1;
return;
elseif(u==2)
   D=dc(u);
dcurrent=D;
   counter=1;
return;
elseif(u==3)
   D=dc(u);
dcurrent=D;
end
```

```
end
            D=alpha_pos;
dcurrent=D;
            counter=1;
return;
else
    u;
    y='hello';
    D=0.1;

end
end
function D1=pos_up(l,alpha_pos,D_cur,beta_pos,delta_pos)
if(l>=5)
    l=5;
end
a=2-2*(l/5);
   r1=rand();
   r2=rand();
    A1=2*a*r1-a;
    C1=2*r2;
D_alpha=abs(C1*alpha_pos-D_cur(kk));
    X1=alpha_pos-A1*D_alpha;
     r1=rand();
   r2=rand();
    A2=2*a*r1-a;
    C2=2*r2;
D_beta=abs(C2*beta_pos-D_cur(kk));
    X2=beta_pos-A2*D_beta;
    r1=rand();
   r2=rand();
    A3=2*a*r1-a;
    C3=2*r2;
D_delta=abs(C3*delta_pos-D_cur(kk));
    X3=delta_pos-A3*D_delta;

    X4=(X1+X2+X3)/3;
    D1(kk)=X4;
if(D1(kk)>0.95)
        D1(kk)=0.55;
elseif (D1(kk)<0.01)
        D1(kk)=0.51;
end
end
disp(D1);
end
```